MSC-01542

NATIONAL AERONAUTICS AND SPACE ADMINISTRATION

NASA GENERAL WORKING PAPER

A PRELIMINARY STRUCTURAL ANALYSIS OF SPACE-BASE LIVING QUARTERS MODULES TO VERIFY A WEIGHT-ESTIMATING TECHNIQUE

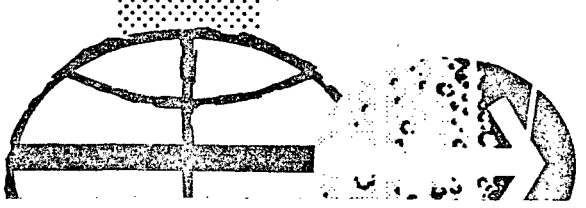

MANNED SPACECRAFT CENTER

HOUSTON, TEXAS

MSC-01542

NASA GENERAL WORKING PAPER

A PRELIMINARY STRUCTURAL ANALYSIS OF SPACE BASE LIVING QUARTERS MODULES TO VERIFY A WEIGHT-ESTIMATING TECHNIQUE

PREPARED BY

David S. Grissom
Spacecraft Design Office

William C. Schneider
Spacecraft Design Office

AUTHORIZED FOR DISTRIBUTION

for Maxime A. Faget
Director of Engineering and Development

NATIONAL AERONAUTICS AND SPACE ADMINISTRATION
MANNED SPACECRAFT CENTER
HOUSTON, TEXAS

CONTENTS

TABLES

FIGURES

A PRELIMINARY STRUCTURAL ANALYSIS OF SPACE-BASE LIVING QUARTERS MODULES TO VERIFY A WEIGHT-ESTIMATING TECHNIQUE

By David S. Grissom and William C. Schneider

1.0 SUMMARY

The determination of a base-line (minimum weight) design for the primary structure of the living quarters modules in an earth-orbiting space base has been investigated. Although the design is preliminary in nature, the supporting analysis is sufficiently thorough to provide a reasonably accurate weight estimate of the major components that are considered to comprise the structural weight of the space base.

2.0 INTRODUCTION

The first phase in the preparation of any efficient design is the establishment of a base-line design on which additions and refinements are made. The design of a space base is no exception. Presented in this report is the configuration that was considered and the preliminary analysis that was performed to determine a structural design for living quarters modules LQM 1 and LQM 2 of an earth-orbiting space base (fig. 1). The purpose of the analysis is to verify a weight-estimating technique.

A detailed library search was performed so that ideas of recognized authorities in the design of large spacecraft structures could be incorporated into this design study. Current articles that contain both theoretical and experimental data concerning crack propagation, optimum pressure-vessel design, and buckling of large spacecraft structures were collected and studied.

Because of the early initiation of this design and analysis effort, little definition of the criteria that would influence the final design was available. Specifically, thermal-control and meteoroid-protection systems had not been established. This study, of necessity, does not incorporate the strength of these systems into the primary structural design. Launch loads were estimated, but the internal loadings (equipment distributions) for each floor were assumed to be equal and distributed uniformly. Other omissions are equipment hard points, windows, hatches, and docking rings. These omissions are estimated to comprise approximately 30 percent of the total structural weight. Operating pressure was specified as 14.65 psia, and the pressure-vessel-wall thickness was adjusted by a scratch factor to correct for scratch depths of 20 percent. In addition to the standard operating configuration in which the two modules and the tunnel act in combination, it was necessary for safety to be able to pressurize each module and the tunnel individually.

The determination of the optimum section for the outer cylindrical wall of LQM 1 and LQM 2 is outlined in section 4.0 of this report. Section 5.0 of the report concerns the establishment of flooring of the two modules. In section 6.0, the tunnel is considered. The analysis that was performed on the end bulkheads for both modules is presented in section 7.0.

3.0 SYMBOLS

A	area
a	ellipse semimajor axis
B	bending stiffness
b	ellipse semiminor axis
C	Euler column coefficient of fixity
C'	constant of integration
D	flexural rigidity
d	width
dF	infinitesimal element of force
dr	infinitesimal element of radius
dθ	infinitesimal element of angle
E	modulus of elasticity
e	extended length
F	force
fs	factor of safety
G	shear modulus of elasticity
g,g'	reference points
H	buckling stress coefficient
h	height
I	area moment of inertia
K	constant
Kl	stress intensity factor
Kc	panel buckling coefficient

k	dimensionless parameter
L	tunnel length
l	length
l'	floor spacing
M	moment
m	dimensionless parameter
N	normal loading per unit length
n	number (quantity)
P	perimeter
p	pressure
Q	shear loading per unit length
$q\alpha$	dynamic pressure times angle of attack
R	reaction forces
r	radius
S	section modulus
S'	transverse shear stiffness
sf	scratch factor
t	thickness
$\bar{t}$	equivalent thickness
u	stringer spacing, beam spacing
V	shear force
W	weight
w	loading per unit length
x,y	variable dimensions

x',y'	ellipse coordinates
Z	curvature parameter
z	coordinate normal to sandwich faces
α	plate parameter for shear
β	plate parameter for bending
γ	one-half length of crack
γ'	plate parameter
Δ	change in
δ	deflection
θ	angle
ν	Poisson ratio
ρ	density
σ	normal stress
τ	shear stress
ϕ	angle

Subscripts:

app	applied
c	core
cr	critical
f	face sheet
h	horizontal
i	inside
k	floor number
l	longitudinal

max.	maximum
min.	minimum
o	outside
s	surface
skin	pressure skin
str	stringer
T	torus
u	ultimate
v	vertical
x	variable
y	yield
θ	hoop
ϕ	meridional

4.0 OUTER CYLINDRICAL WALL

The computation of the outer wall dimensions for each floor included consideration of the loads, which consist of free-standing ground winds, maximum $q\alpha$, first-stage end boost, and internal pressure. The main structural purposes of the wall are to hold internal pressure and to prevent buckling during the maximum loading conditions. The wall consists of a pressure skin reinforced by longitudinal stringers and circumferential rings. This configuration was chosen because it was considered to be efficient, lightweight, and proven. A monocoque shell with longitudinal stringers and circumferential rings has been reported to be the most efficient type of structure for this application. From figure 2, it is evident that the skin-stringer-ring construction is the most efficient. Sandwich construction is slightly less efficient (ref. 1).

The stringers are placed on the external side of the pressure skin because cylindrical shells stiffened by external stringers have been shown to exhibit, for some geometrics, as much as two times the buckling load capability as cylindrical shells stiffened with internal stringers (refs. 2 and 3). The design configuration presented in this report has rings only at the floor levels, but the rings are placed such that the ring center of gravity is external to the skin. A later design optimization possibly could be obtained by the addition of small rings between the floors; however, this optimization was not considered for this report.

The skin is designed to withstand internal pressure. The stringer spacing is determined such that the skin is between stringers at the point of buckling. The stringers are designed so that the stringers and the skin will just withstand the induced compression loads without buckling. A safety factor of 2 was used for buckling loads, and a safety factor of 1 was used for tensile stress compared with yield stress. The design analyses of LQM 1 and LQM 2 are discussed separately.

4.1 LIVING QUARTERS MODULE 1

The outer wall of LQM 1 is a conical frustrum in which the smaller end is attached to a cylinder. Living quarters module 1 and the numbering system for the stringers between floors are shown in figure 1. No floor exists at levels -4, -5, and -6; only rings are used as stiffeners. In this section of the report, the design loads are determined, the pressure-skin thickness is calculated, the stringer spacing is computed, the optimum stringer section is determined, and the total weight of the skin and stringers is calculated for each floor of LQM 1 of the space base.

4.1.1 External Loads

The external loads for LQM 1 were computed by Structures and Mechanics Division personnel. The three loading cases considered are free-standing ground winds, maximum product of dynamic pressure and angle of attack $q\alpha$, and first-stage end boost. The external loads for each floor of LQM 1 are presented in table I.

4.1.2 Internal Pressure Loads

During launch of the space base, the ambient external pressure decreases and the internal pressure remains constant. Therefore, a differential pressure is induced across the pressure wall and causes a tension load in the axial direction that decreases the axial-compressive buckling load. The hoop tension load in the cylinder wall that is caused by this differential pressure is not computed.

The following is the derivation for the load per inch on the inner and outer cylinder (fig. 3) that is caused by internal pressure.

$$\Sigma F \Longrightarrow dF_o + dF_i = \int_{r_i}^{r_o} r \, d\theta \, dr \, p$$

$$dF_o + dF_i = p \frac{d\theta}{2} \left(r_o^2 - r_i^2 \right) \tag{1}$$

$$\Sigma M \text{ (about the diameter)} \Longrightarrow dF_o \, r_o + dF_i \, r_i = \int_{r_i}^{r_o} r(r \, d\theta) dr \, p$$

$$dF_o \, r_o + dF_i \, r_i = \frac{p \, d\theta}{3} \left(r_o^3 - r_i^3 \right) \tag{2}$$

Solving equations (1) and (2) for dF_o and dF_i yields

$$dF_o = p\, d\theta \frac{\left[-\frac{r_i}{2}\left(r_o^2 - r_i^2\right) + \frac{1}{3}\left(r_o^3 - r_i^3\right)\right]}{r_o - r_i}$$

$$dF_i = p\, d\theta \frac{\left[-\frac{\left(r_o^3 - r_i^3\right)}{3} + \frac{r_o}{2}\left(r_o^2 - r_i^2\right)\right]}{r_o - r_i}$$

The load per inch is $N_o = dF_o/r_o\, d\theta$ and $N_i = dF_i/r_i\, d\theta$. Therefore

$$N_o = \frac{2r_o + r_i}{r_o}\left[(r_o - r_i)\frac{p}{6}\right]$$

$$N_i = \frac{2r_i + r_o}{r_i}\left[(r_o - r_i)\frac{p}{6}\right]$$

calculated values of N_o/p for each floor are shown in table II. The differential pressures p for the various loading conditions are 0 psi for case I, 11 psi for case II, and 14.65 psi for case III.

4.1.3 Total Resultant Load in the Wall

The total resultant load in the wall is comprised of the axial compression load, the tension and compression loads caused by the moment, and the tension load caused by differential pressure. The total resultant load per inch of circumference can be written as

$$N_k = K_k p - \frac{\text{axial load}}{2\pi r_o} \pm \frac{M_k}{\pi r_o^2}$$

where $K = N_o/p$ and M = moment.

For case I, the total resultant load (in pounds per inch of circumference) is determined for each floor and ring by using the moment and axial-load values (table I) and $p = 0$ psi.

Floor 3:

$$N_3 = 52.2(0)\ \frac{-23 \times 10^4}{2\pi(178)} \pm \frac{33 \times 10^6}{\pi(178)^2}$$

$$N_3 = \begin{cases} -536 \\ +126 \end{cases}$$

Floor 2:

$$N_2 = 48.3(0) - \frac{17 \times 10^4}{2\pi(167)} \pm \frac{26 \times 10^6}{\pi(167)^2}$$

$$N_2 = \begin{cases} -458 \\ +134 \end{cases}$$

Floor 1:

$$N_1 = 42.9(0) - \frac{11 \times 10^4}{2\pi(151)} \pm \frac{20 \times 10^6}{\pi(151)^2}$$

$$N_1 = \begin{cases} -394.3 \\ +163.3 \end{cases}$$

Floor 0:

$$N_0 = 39.8(0) - \frac{8 \times 10^4}{2\pi(142)} \pm \frac{16 \times 10^6}{\pi(142)^2}$$

$$N_0 = \begin{cases} -342 \\ +163 \end{cases}$$

Floor -1:

$$N_{-1} = 36.4(0) - \frac{7 \times 10^4}{2\pi(132)} \pm \frac{12 \times 10^6}{\pi(132)^2}$$

$$N_{-1} = \begin{cases} -302 \\ +135 \end{cases}$$

Floor -2:

$$N_{-2} = 32.8(0) - \frac{4 \times 10^4}{2\pi(122)} \pm \frac{8 \times 10^6}{\pi(122)^2}$$

$$N_{-2} = \begin{cases} -223 \\ +118.6 \end{cases}$$

Floor -3:

$$N_{-3} = 21.9(0) - \frac{3 \times 10^4}{2\pi(91)} \pm \frac{6 \times 10^6}{\pi(91)^2}$$

$$N_{-3} = \begin{cases} -281 \\ +178 \end{cases}$$

Ring -4:

$$N_{-4} = 21.9(0) - \frac{2.8 \times 10^4}{2\pi(91)} \pm \frac{4 \times 10^6}{\pi(91)^2}$$

$$N_{-4} = \begin{cases} -202.7 \\ +104.9 \end{cases}$$

Ring -5:

$$N_{-5} = 21.9(0) - \frac{2.7 \times 10^4}{2\pi(91)} \pm \frac{2 \times 10^6}{\pi(91)^2}$$

$$N_{-5} = \begin{cases} -124.1 \\ +29.7 \end{cases}$$

Ring -6:

$$N_{-6} = 21.9(0) - \frac{1.8 \times 10^4}{2\pi(91)} \pm \frac{1 \times 10^6}{\pi(91)^2}$$

$$N_{-6} = \begin{cases} -69.8 \\ +7 \end{cases}$$

For case II, the total resultant load (in pounds per inch of circumference) is determined for each floor and ring by using the moment and axial-load values (table I) and $p = 11$ psi.

Floor 3:

$$N_3 = 52.2(11) - \frac{9.2 \times 10^5}{2\pi(178)} \pm \frac{27.5 \times 10^7}{\pi(178)^2}$$

$$N_3 = \begin{cases} -3038 \\ +2540 \end{cases}$$

Floor 2:

$$N_2 = 48.3(11) - \frac{8.25 \times 10^5}{2\pi(167)} \pm \frac{19.5 \times 10^7}{\pi(167)^2}$$

$$N_2 = \begin{cases} -2481 \\ +1990 \end{cases}$$

Floor 1:

$$N_1 = 42.9(11) - \frac{7.5 \times 10^5}{2\pi(151)} \pm \frac{15.7 \times 10^7}{\pi(151)^2}$$

$$N_1 = \begin{cases} -2518.8 \\ +1880.8 \end{cases}$$

Floor 0:

$$N_0 = 39.8(11) - \frac{6.2 \times 10^5}{2\pi(142)} \pm \frac{12 \times 10^7}{\pi(142)^2}$$

$$N_0 = \begin{cases} -2152 \\ +1637 \end{cases}$$

Floor -1:

$$N_{-1} = 36.4(11) - \frac{4.5 \times 10^5}{2\pi(132)} \pm \frac{9 \times 10^7}{\pi(132)^2}$$

$$N_{-1} = \begin{cases} -1786.8 \\ +1503 \end{cases}$$

Floor -2:

$$N_{-2} = 32.8(11) - \frac{3 \times 10^5}{2\pi(122)} \pm \frac{6.75 \times 10^7}{\pi(122)^2}$$

$$N_{-2} = \begin{cases} -1474 \\ +1414 \end{cases}$$

Floor -3:

$$N_{-3} = 21.9(11) - \frac{2 \times 10^5}{2\pi(91)} \pm \frac{4.5 \times 10^7}{\pi(91)^2}$$

$$N_{-3} = \begin{cases} -1798.3 \\ +1662 \end{cases}$$

Ring -4:

$$N_{-4} = 21.9(11) - \frac{1 \times 10^5}{2\pi(91)} \pm \frac{3.75 \times 10^7}{\pi(91)^2}$$

$$N_{-4} = \begin{cases} -1335 \\ +1548 \end{cases}$$

Ring -5:

$$N_{-5} = 21.9(11) - \frac{7 \times 10^4}{2\pi(91)} \pm \frac{2.25 \times 10^7}{\pi(91)^2}$$

$$N_{-5} = \begin{cases} -695 \\ +1014 \end{cases}$$

Ring -6:

$$N_{-6} = 21.9(11) - \frac{7 \times 10^4}{2\pi(91)} \pm \frac{1.5 \times 10^7}{\pi(91)^2}$$

$$N_{-6} = \begin{cases} -410 \\ +729 \end{cases}$$

For case III, the total resultant load (in pounds per inch of circumference) is determined for each floor and ring by using the moment and axial-load values (table I) and $p = 14.65$ psi.

Floor 3:

$$N_3 = 52.2(14.65) - \frac{11.5 \times 10}{2\pi(178)} \pm \frac{6.2 \times 10^6}{\pi(178)^2}$$

$$N_3 = \begin{cases} -321 \\ +0 \end{cases}$$

Floor 2:

$$N_2 = 48.3(14.65) - \frac{8.5 \times 10^5}{2\pi(167)} \pm \frac{4.25 \times 10^6}{\pi(167)^2}$$

$$N_2 = \begin{cases} -151 \\ +0 \end{cases}$$

Floor 1:

$$N_1 = 42.9(14.65) - \frac{5.05 \times 10^5}{2\pi(151)} \pm \frac{2.75 \times 10^6}{\pi(151)^2}$$

$$N_1 = \begin{cases} -0 \\ +134 \end{cases}$$

Floor 0:

$$N_0 = 39.8(14.65) - \frac{4 \times 10^5}{2\pi(142)} \pm \frac{2 \times 10^6}{\pi(142)^2}$$

$$N_0 = \begin{cases} -0 \\ +164 \end{cases}$$

Floor -1:

$$N_{-1} = 36.4(14.65) - \frac{3 \times 10^5}{2\pi(132)} \pm \frac{1.2 \times 10^6}{\pi(132)^2}$$

$$N_{-1} = \begin{cases} -0 \\ +191 \end{cases}$$

Floor -2:

$$N_{-2} = 32.8(14.65) - \frac{2 \times 10^5}{2\pi(122)} \pm \frac{1 \times 10^6}{\pi(122)^2}$$

$$N_{-2} = \begin{cases} -0 \\ +239 \end{cases}$$

Floor -3:

$$N_{-3} = 21.9(14.65) - \frac{1.6 \times 10^5}{2\pi(91)} \pm \frac{7.5 \times 10^5}{\pi(91)^2}$$

$$N_{-3} = \begin{cases} -0 \\ +69 \end{cases}$$

Ring -4:

$$N_{-4} = 21.9(14.65) - \frac{1.2 \times 10^5}{2\pi(91)} \pm \frac{2.5 \times 10^5}{\pi(91)^2}$$

$$N_{-4} = \begin{cases} -0 \\ +119.7 \end{cases}$$

Ring -5:

$$N_{-5} = 21.9(14.65) - \frac{1 \times 10^5}{2\pi(91)} \pm \frac{1 \times 10^5}{\pi(91)^2}$$

$$N_{-5} = \begin{cases} -0 \\ +148.8 \end{cases}$$

Ring -6:

$$N_{-6} = 21.9(14.65) - \frac{5 \times 10^4}{2\pi(91)}$$

$$N_{-6} = \begin{cases} -0 \\ +232 \end{cases}$$

4.1.4 Limit Loads

The limit loads are the maximum loads expected on a particular floor. The limit load for each floor is shown in table III.

4.1.5 Design Loads

The design loads are obtained by multiplying the limit loads by the appropriate safety factor. The safety factors for compressive buckling loads and for tension loads are 2 and 1.5, respectively. The design loads for compression and tension are given in table IV.

4.1.6 Pressure-Skin Thickness

The following design requirements were considered for the design of the thin pressure skin.

a. The internal limit pressure shall be 14.65 psig.

b. An explosive failure shall not occur if a scratch that is as deep as 20 percent of material thickness and 6 inches long exists in the skin.

c. Cracks shall not propagate.

d. The working stress factor of safety shall be 1.5 times the allowable yield stress.

The material considered for the pressure skin was 2219-T87 aluminum, which has a welded strength of σ_u = 41 000 psi and σ_y = 30 000 psi.

The thickness required for crack-propagation prevention is calculated in the following manner. The tangential stress in a thin-walled cylindrical pressure vessel is $\sigma = p \frac{r_o}{t}$. If a crack 6 inches long shall not propagate (ref. 4, fig. 4), then $K1 = \sigma\sqrt{\pi\gamma}$. Where $\gamma = 3$ inches, $p = 14.65$ psi, and $2 r_o = 372$ inches, then

$$K1 = \frac{(1.5)(14.7)(372)}{2t} \sqrt{\pi 3} \leq 69\ 000$$

and

$$t \geq 0.182 \text{ in.}$$

A skin thickness is required that will provide acceptable strength even if a scratch penetrates to a depth of 20 percent of the material thickness. This thickness is calculated as follows.

$$\sigma = \frac{pr_o}{0.8t} = (1.5) \frac{(14.65)(372)}{2(0.8)t} = \frac{5105.7}{t}$$

$$\sigma_y = 30\ 000 \text{ psi}$$

The requirement is

$$\sigma \leq \sigma_y \Longrightarrow \frac{5105.7}{t} \leq 30\ 000$$

Therefore

$$t \geq 0.170 \text{ in.}$$

The requirements for both crack prevention and scratch strength are satisfied by a thickness of 0.182 inch.

4.1.7 Stringer Spacing

The distance between the longitudinal stringers for each floor is determined such that the thin skin between stringers is on the verge of buckling. The allowable axial-compressive buckling stress for a curved panel is increased by internal pressure.

To determine the increase in allowable buckling stress caused by internal pressure, the following parameter is computed. The computation for floor 3 is presented as an example.

$$\frac{p}{E}\left(\frac{r_o}{t}\right)^2 = \frac{(11)(178)^2}{10^7(0.182)} = 1.1$$

Using this parameter and the curve shown in figure 5 (ref. 5), the increase in allowable buckling stress is computed as follows.

$$\Delta H = 0.45$$

$$\Delta\sigma_{cr} = \Delta H \frac{Et}{r_o} = \frac{(0.45)10^7(0.182)}{178}$$

$$\Delta\sigma_{cr} = 4259 \text{ psi}$$

The total allowable buckling stress is given by

$$\sigma_{cr} = \frac{Kc\pi^2 Et^2}{12(1 - \nu^2)u^2} + \Delta\sigma_{cr}$$

The applied stress should be less than or equal to the critical stress.

$$\sigma_{app} \leq \sigma_{cr}$$

The ratio of the loading per inch of circumference to the skin thickness for floor 3 is

$$\frac{N_3}{t} = \frac{6076}{0.182} = 33\ 384 \leq \frac{Kc}{u^2}\left[\frac{\pi^2(0.182)^2 10^7}{12(0.91)}\right] + 4259$$

$$29\ 125 \leq 2.828 \times 10^5 \frac{Kc}{u^2}$$

Therefore

$$u^2 \leq 9.58Kc \tag{3}$$

The curvature parameter Z is given by

$$Z = \frac{u^2(1 - \nu^2)^{1/2}}{r_o t} \tag{4}$$

Therefore

$$Z = 0.03u^2$$

For the iterative procedure that is used to determine the stringer spacing u, (1) assume Kc and determine u from inequality (3); (2) with this value of u, determine Z from equation (4); (3) with this value of Z and figure 6 (ref. 5), read the corrected value of Kc.

These three steps are repeated until convergence is reached at which point the value of u is established.

Let

$$Kc = 4 \Longrightarrow u = 6.169 \text{ in.} \Longrightarrow Z = 1.419 \Longrightarrow Kc = 7 \Longrightarrow u = 8.16 \text{ in.}$$

The number of stringers needed is the next integer greater than the ratio of circumference to u. Similar calculations were performed for each floor; the results are presented in table V.

4.1.8 Determination of the Stringer Cross Section

The optimum wide-flange cross section is computed for each floor of LQM 1 by first determining the approximate area moment of inertia needed to withstand the applied loads at each floor. With this determination, the moment of inertia (just smaller than the moment of inertia that is needed) is found by consulting the standard wide-flange tables. Next, the length that must be added to the flange to give the exact inertia and area required to withstand the applied loads is determined.

The critical buckling load per inch for this stringer-stiffened structure is given (ref. 6) as

$$N_{cr} = \frac{C\pi^2 EI}{(l')^2} + \frac{Et\sqrt{t\bar{t}}}{\sqrt{3}\, r_o}$$

where $C = 1$

$l' = 108$ in.

$E = 1 \times 10^7$ psi

$t = 0.182$ in.

and

$$\bar{t} = t_s + \frac{A_{str}}{u} \qquad I_t = \left(\frac{I_{str}}{u} + \frac{t_s^3}{12}\right)$$

Therefore

$$N_{cr} = 8453 I_t + 2410\sqrt{\bar{t}}$$

Floor 3:

If $r_o = 178$ inches, $N_{app} = 6076$ pounds per inch, and $u = 8.15$ inches, then

$$6076 \leq 8453\left(\frac{I_{str}}{8.15} + 0.0005\right) + 2410\sqrt{0.182 + \left(\frac{A_{str}}{8.15}\right)}$$

$$6072 \leq 1037 I_{str} + 2410\sqrt{0.182 + \left(\frac{A_{str}}{8.15}\right)}$$

Therefore

$$I_{str} \geq 4.86 \text{ in}^4$$

Let

$$I_{str} = 6.968 + 3.52x$$

$$A_{str} = 2.60 + x$$

$$6072 \leq 7225.8 + 3650x + 2410\sqrt{0.50 + 0.122x}$$

$$x \geq -0.316 - 0.660\sqrt{.05 + 0.122x}$$

$$x \geq -0.74 \text{ in.}$$

Therefore

$$I_3 = 4.367 \text{ in}^4$$

$$A_3 = 1.86 \text{ in}^2$$

Floor 2:

If $r_o = 167$ inches, $N_{app} = 4962$ pounds per inch, and $u = 9.2$ inches, then

$$4962 \leq 8453\left(\frac{I_{str}}{9.2} + 0.0005\right) + (2410)\frac{178}{167}\sqrt{0.182 + \left(\frac{A_{str}}{9.2}\right)}$$

$$4962 \leq 918.8I_{str} + 4.226 + 2568\sqrt{0.182 + \left(\frac{A_{str}}{9.2}\right)}$$

Let $I_{str} = 6.968 + 3.52x$

$A_{str} = 2.60 + x$

$$4962 \leq 6402 + 3234x + 4.226 + 2568\sqrt{0.46 + 0.1x}$$

$$x \geq -0.45 - 0.79\sqrt{0.46 + 0.1x}$$

$$x \geq -0.93 \text{ in.}$$

Therefore

$$I_2 = 3.69 \text{ in}^4$$

$$A_2 = 1.67 \text{ in}^2$$

Floor 1:

If $r_o = 151$ inches, $N_{app} = 5036$ pounds per inch, and $u = 9.2$ inches, then

$$5036 \leq 8453\left(\frac{I_{str}}{9.2} + 0.0005\right) + (2410)\frac{178}{151}\sqrt{0.46 + 0.1x}$$

$$5036 \leq 918.8I_{str} + 4.22 + 2829\sqrt{0.46 + 0.1x}$$

If I_{str} and A_{str} are the same as those for floors 2 and 3

$$5036 \leq 918.8\ (6.968 + 3.5x) + 4.2 + 2.829\sqrt{0.46 + 0.1x}$$

$$5036 \leq 6402 + 3215.8x + 4.2 + 2829\sqrt{0.46 + 0.1x}$$

$$x \geq -0.426 - 0.87\sqrt{0.46 + 0.1x}$$

$$x \geq 0.95 \text{ in.}$$

Therefore

$$I_1 = 3.62 \text{ in}^4$$

$$A_1 = 1.65 \text{ in}^2$$

Floor 0:

If $r_o = 142$ inches, $N_{app} = 4304$ pounds per inch, and $u = 9.9$ inches, then

$$4304 \leq 8453\left(\frac{I_{str}}{9.9} + 0.0005\right) + (2410)\frac{178}{142}\sqrt{0.182 + \left(\frac{A_{str}}{9.9}\right)}$$

$$4304 \leq 853.8I_{str} + 4.2 + 3020\sqrt{0.182 + \left(\frac{A_{str}}{9.9}\right)}$$

Let $I_{str} = 4.136 + 2.12x$

$A_{str} = 1.521 + 0.624x$

$$4304 \leq 3531 + 1810x + 4.2 + 3020\sqrt{0.335 + 0.06x}$$

$$x \geq +0.42 - 1.66\sqrt{0.335 + 0.06x}$$

$$x \geq -0.49 \text{ in.}$$

Therefore

$$I_o = 3.082 \text{ in}^4$$

$$A_o = 1.21 \text{ in}^2$$

Floor -1:

If $r_o = 132$ inches, $N_{app} = 3572$ pounds per inch, and $u = 11.7$ inches, then

$$3572 \leq 8453 \left(\frac{I_{str}}{11.7}\right) + 4.2 + (2410) \frac{178}{132} \sqrt{0.182 + \left(\frac{A_{str}}{11.7}\right)}$$

$$3572 \leq 722.5 I_{str} + 4.2 + 3249 \sqrt{0.182 + \left(\frac{A_{str}}{11.7}\right)}$$

If the equations for I_{str} and A_{str} are the same as those for floor 0

$$3572 \leq 722.5(4.136 + 2.12x) + 4.2 + 3249 \sqrt{0.312 + 0.05x}$$

$$3572 \leq 2988.3 + 1532x + 4.2 + 3249 \sqrt{0.312 + 0.05x}$$

$$x \geq 0.378 - 2.12 \sqrt{0.312 + 0.05x}$$

$$x \geq -0.73 \text{ in.}$$

Therefore

$$I_{-1} = 2.57 \text{ in}^4$$

$$A_{-1} = 1.065 \text{ in}^2$$

Floor -2:

If $r_o = 122$ inches, $N_{app} = 2948$ pounds per inch, and $u = 17.03$ inches, then

$$2948 \leq 8453 \left(\frac{I_{str}}{17.03}\right) + 4.2 + (2410)\frac{178}{122}\sqrt{0.182 + \left(\frac{A_{str}}{17.03}\right)}$$

Let $I_{str} = 2.424 + 1.87x$

$A_{str} = 0.969 + 0.5x$

$$2948 \leq 496.4\ (2.424 + 1.87x) + 4.2 + 3516\sqrt{0.182 + \left(\frac{0.969 + 0.5x}{17.03}\right)}$$

$$2948 \leq 1203 + 928x + 4.2 + 3516\sqrt{0.23 + 0.029x}$$

$$x \geq 1.875 - 3.79\sqrt{0.23 + 0.029x}$$

$$x \geq 0.05 \text{ in.}$$

Therefore

$$I_{-2} = 2.424 \text{ in}^4$$

$$A_{-2} = 0.969 \text{ in}^2$$

Floor -3:

If $r_o = 91$ inches, $N_{app} = 3596$ pounds per inch, $u = 11.9$ inches, and if the equations for I_{str} and A_{str} are the same as those for floor -2, then

$$3596 \leq 710(2.424 + 1.87x) + 4.2 + 4714\sqrt{0.263 + 0.042x}$$

$$x \geq 1.4 - 3.55\sqrt{0.263 + 0.042x}$$

$$x \geq 0.36 \text{ in.}$$

Therefore

$$I_{-3} = 1.73 \text{ in}^4$$

$$A_{-3} = 0.78 \text{ in}^2$$

Ring -4:

If $r_o = 91$ inches, $N_{app} = 2670$ pounds per inch, and $u = 15.5$ inches, then

$$2670 \leq 8453 \left(\frac{I_{str}}{15.5}\right) + 4.2 + (2410)\frac{178}{91}\sqrt{0.182 + \left(\frac{0.851 + 0.5x}{15.5}\right)}$$

Let $I_{str} = 1.262 + 1.03x$

$A_{str} = 0.851 + 0.5x$

$$2670 \leq 480(1.262 + 1.03x) + 4.2 + 4714\sqrt{0.182 + \left(\frac{0.851 + 0.5x}{15.5}\right)}$$

$$2670 \leq 605 + 494x + 4.2 + 4714\sqrt{0.237 + 0.03x}$$

$$x \geq 4.17 - 9.54\sqrt{0.237 + 0.03x}$$

$$x \geq -0.36$$

Therefore

$$I_{-4} = 0.89 \text{ in}^4$$

$$A_{-4} = 0.67 \text{ in}^2$$

Ring -5:

If $r_o = 91$ inches, $N_{app} = 1390$ pounds per inch, and $u = 16.8$ inches, then

$$1390 \leq 503I_{str} + 4.2 + 4714\sqrt{0.182 + \left(\frac{A_{str}}{16.8}\right)}$$

No stringer is needed $\left(I_{str} = 0 \text{ and } A_{str} = 0\right)$ because the inequality is satisfied identically.

Ring -6:

If r_o = 91 inches, N_{app} = 820 pounds per inch, and u = 16.8 inches, then

$$820 \leq 503I_{str} + 4.2 + 4714\sqrt{0.182 + \left(\frac{A_{str}}{16.8}\right)}$$

No stringer is needed because the inequality is satisfied identically for $I_{str} = 0$ and $A_{str} = 0$. The results of the computations for the stringer cross sections and the weights of the stringers are presented in table VI. The weight of the pressure skin is

$$W_{skin} = 2\pi(0.182)(0.1)[90(372) + (108.5)(696)]$$

$$W_{skin} = 12\ 457 \text{ lb}$$

The total weight of the primary external LQM 1 structure (pressure-skin weight plus stringer weight) is 22 056 pounds.

4.2 LIVING QUARTERS MODULE 2

The outer wall of LQM 2 is cylindrical. Living quarters module 2 and the numbering system for the stringers between floors are shown in figure 1. In this section of the report, the design loads are determined, the stringer spacing is computed, the optimum stringer section is determined, and the total weight of the skin and stringers is calculated for each floor of LQM 2 of the space base.

4.2.1 External Loads

The external loads for LQM 2 were computed by Structures and Mechanics Division personnel. The three loading cases that were considered for LQM 1 also were considered for LQM 2. The external loads for each floor of LQM 2 are presented in table VII.

4.2.2 Internal Pressure Loads

The relation for axial tension in the outside wall was given previously as

$$N_o = \frac{2r_o + r_i}{r_o}\left[(r_o - r_i)\frac{p}{6}\right]$$

For this cylindrical shape, r_o is not different at each floor. Consequently, if $r_i = 36$ inches and $r_o = 186$ inches, then $N_o = 54.8p$. The differential pressures p for the various loading conditions are 0 psi for case I, 11 psi for case II, and 14.65 psi for case III.

4.2.3 Total Resultant Load in the Wall

The total resultant load per inch of circumference can be written as

$$N_k = 54.8p - \frac{\text{axial load}}{2\pi r_o} \pm \frac{M_k}{\pi r_o^2}$$

For case I, the total resultant load (in pounds per inch of circumference) is determined for each floor by using the moment and axial-load values (table VII) and $p = 0$ psi.

Floor 5:

$$N_5 = 0 - \frac{2.2 \times 10^5}{1168} \pm \frac{4.1 \times 10^7}{0.01 \times 10^7}$$

$$N_5 = \begin{cases} -221.6 \\ +598.4 \end{cases}$$

Floor 4:

$$N_4 = 0 - \frac{1.9 \times 10^5}{1168} \pm \frac{3.5 \times 10^7}{0.01 \times 10^7}$$

$$N_4 = \begin{cases} -187 \\ +512.7 \end{cases}$$

Floor 3:

$$N_3 = 0 - \frac{1.3 \times 10^5}{1168} \pm \frac{2.7 \times 10^7}{0.01 \times 10^7}$$

$$N_3 = \begin{cases} -158.6 \\ +381 \end{cases}$$

Floor 2:

$$N_2 = 0 - \frac{1.1 \times 10^5}{1168} \pm \frac{2 \times 10^7}{0.01 \times 10^7}$$

$$N_2 = \begin{cases} -105.8 \\ +294 \end{cases}$$

Floor 1:

$$N_1 = 0 - \frac{0.75 \times 10^5}{1168} \pm \frac{1.1 \times 10^7}{0.01 \times 10^7}$$

$$N_1 = \begin{cases} -46 \\ +174 \end{cases}$$

For case II, the total resultant load (in pounds per inch of circumference) is determined for each floor by using the moment and axial-load values (table VII) and $p = 11$ psi.

Floor 5:

$$N_5 = 54.8(11) - \frac{5.5 \times 10^2}{1.168} \pm \frac{1.75 \times 10^8}{0.001 \times 10^8}$$

$$N_5 = \begin{cases} -1618.1 \\ +1881.9 \end{cases}$$

Floor 4:

$$N_4 = 54.8(11) - \frac{4.8 \times 10^2}{1.168} \pm \frac{1.4 \times 10^8}{0.001 \times 10^8}$$

$$N_4 = \begin{cases} -1208.1 \\ +1591.8 \end{cases}$$

Floor 3:

$$N_3 = 54.8(11) - \frac{4.5 \times 10^2}{1.168} \pm \frac{1.20 \times 10^8}{0.001 \times 10^8}$$

$$N_3 = \begin{cases} -982 \\ +1417 \end{cases}$$

Floor 2:

$$N_2 = 54.8(11) - \frac{3.9 \times 10^2}{1.168} \pm \frac{0.99 \times 10^8}{0.001 \times 10^8}$$

$$N_2 = \begin{cases} -721 \\ +1259 \end{cases}$$

Floor 1:

$$N_1 = 54.8(11) - \frac{3 \times 10^2}{1.168} \pm \frac{0.8 \times 10^8}{0.001 \times 10^8}$$

$$N_1 = \begin{cases} -454 \\ +1146 \end{cases}$$

For case III, the total resultant load (in pounds per inch of circumference) is determined for each floor by using the moment and axial-load values (table VII) and $p = 14.65$ psi.

Floor 5:

$$N_5 = 54.8(14.65) - \frac{1 \times 10^3}{1.168} \pm \frac{6 \times 10^6}{0.1 \times 10^6}$$

$$N_5 = \begin{cases} -116 \\ +3.9 \end{cases}$$

Floor 4:

$$N_4 = 54.8(14.65) - \frac{0.85 \times 10^3}{1.168} \pm \frac{4 \times 10^6}{0.1 \times 10^6}$$

$$N_4 = \begin{cases} -32 \\ +112 \end{cases}$$

Floor 3:

$$N_3 = 54.8(14.65) - \frac{0.75 \times 10^3}{1.168} \pm \frac{3 \times 10^6}{0.1 \times 10^6}$$

$$N_3 = \begin{cases} -0 \\ +188 \end{cases}$$

Floor 2:

$$N_2 = 54.8(14.65) - \frac{0.6 \times 10^3}{1.168} \pm \frac{2 \times 10^6}{0.1 \times 10^6}$$

$$N_2 = \begin{cases} -0 \\ +306 \end{cases}$$

Floor 1:

$$N_1 = 54.8(14.65) - \frac{0.4 \times 10^3}{1.168} \pm \frac{0.9 \times 10^6}{0.1 \times 10^6}$$

$$N_1 = \begin{cases} -0 \\ +636 \end{cases}$$

4.2.4 Limit Loads

The limit loads are the maximum loads expected on a particular floor. The limit loads for each floor are given in table VIII.

4.2.5 Design Loads

Safety factors of 2 and 1.5 are used to compute compressive buckling loads and design tension loads, respectively. The design loads obtained by multiplying the limit load for each floor by the appropriate safety factor are given in table IX.

4.2.6 Pressure-Skin Thickness

The pressure-skin thickness established for LQM 1 is used for the pressure-skin thickness of LQM 2. The requirements for both crack-propagation prevention and scratch strength are satisfied by a thickness of 0.182 inch.

4.2.7 Stringer Spacing

The distance between the longitudinal stringers for each floor is determined such that the skin between the stringers is on the verge of buckling. The allowable axial-compressive buckling stress for a curved panel is increased by internal pressure.

To determine the increase in allowable buckling stress caused by internal pressure, the following parameter is computed.

$$\frac{p}{E}\left(\frac{r_o}{t}\right)^2 = \frac{11}{10^7}\left(\frac{186}{0.182}\right)^2 = 1.215$$

By using this parameter and the curve shown in figure 5 (ref. 5), the increase in allowable buckling stress is computed as follows.

$$\Delta H = 0.45$$

$$\Delta\sigma_{cr} = \frac{\Delta HEt}{r_o} = \frac{(0.45)10^7(0.182)}{186}$$

$$\Delta\sigma_{cr} = 4280$$

The total allowable buckling stress is given by

$$\sigma_{cr} = \frac{Kc\pi^2Et^2}{12(1 - \nu^2)u^2} + \Delta\sigma_{cr}$$

$$\frac{N_k}{t} = \frac{Kc_k}{u_k^2}\left(2.828 \times 10^5\right) + 4280$$

Thus, the following inequalities should hold true for each floor.

Floor 5:

$$\frac{3236}{0.182} \leq \frac{Kc_5}{u_5^2}\left(2.828 \times 10^5\right) + 4280$$

Floor 4:

$$\frac{2416}{0.182} \leq \frac{Kc_4}{u_4^2}\left(2.828 \times 10^5\right) + 4280$$

Floor 3:

$$\frac{1964}{0.182} \leq \frac{Kc_3}{u_3^2}\left(2.828 \times 10^5\right) + 4280$$

Floor 2:

$$\frac{1442}{0.182} \leq \frac{Kc_2}{u_2^2}\left(2.828 \times 10^5\right) + 4280$$

Floor 1:

$$\frac{908}{0.182} \leq \frac{Kc_1}{u_1^2}\left(2.828 \times 10^5\right) + 4280$$

These inequalities can be reduced to the following inequalities.

$$u_5^2 \leq 20.19Kc_5$$

$$u_4^2 \leq 30.18Kc_4$$

$$u_3^2 \leq 41.5Kc_3$$

$$u_2^2 \leq 73.15Kc_2$$

$$u_1^2 \leq 333Kc_1$$

The curvature parameter Z is given by

$$Z_k = \frac{u_k^2 \left(1 - \nu^2\right)^{1/2}}{r_o t}$$

$$Z_k = 0.03 u_k^2$$

By using the preceding inequalities and the equation for Z with figure 6 (ref. 5), the spacing u (in inches) for each floor can be computed.

$$u_5 \leq 11$$

$$u_4 \leq 13.4$$

$$u_3 \leq 15.7$$

$$u_2 \leq 21.8$$

No stringer is required for floor 1.

The circumference of the cylinder is 1168 inches. Therefore, if an integer number of stringers is to be placed at each floor, the values of u_k will be increased slightly. The number of stringers and the stringer spacing for each floor are given in table X.

4.2.8 Determination of the Stringer Cross Section

The same method used to compute the optimum wide-flange cross section for each floor of LQM 1 is used to compute the LQM 2 stringer cross sections. Hence

$$N_{cr} = \frac{C\pi^2 EI}{(l')^2} + \frac{Et\sqrt{t\bar{t}}}{\sqrt{3}r_o}$$

where $C = 1$

$l' = 108$ in.

$E = 1 \times 10^7$ psi

$t = 0.182$ in.

and

$$\bar{t} = t_s + \frac{A_{str}}{u} \qquad I_t = \left(\frac{I_{str}}{u} + \frac{t_s^3}{12}\right)$$

Therefore

$$N_{cr} = 8453 I_t + 2410\sqrt{\bar{t}}$$

Floor 5:

If $r_o = 186$ inches, $N_{app} = 3236$ pounds per inch, and $u = 10.9$ inches, then

$$3236 \leq 46.49 + \frac{8453}{10.9} I_{str} + 2311\sqrt{0.182 + \left(\frac{A_{str}}{10.9}\right)}$$

Because a 4- by 2-inch wide-flange beam (ref. 7) gives $I = 2.424$ and $A = 0.969$, a length of $2x$ is added to each flange. The resulting section properties are as follows.

$$I_{str} = 2.424 + 1.877x$$

$$A_{str} = 0.969 + 0.5x$$

Therefore

$$3189.5 \leq 775.5(2.424 + 1.877x) + 2311\sqrt{0.2658 + 0.045x}$$

The solution for x from the inequality is

$$x \geq 0.076 \text{ in.}$$

Therefore

$$I_5 = 2.56 \text{ in}^4$$

$$A_5 = 1.007 \text{ in}^2$$

Floor 4:

If $r_o = 186$ inches, $N_{app} = 2416$ pounds per inch, and $u_4 = 13.3$ inches, then

$$2416 \leq 46.49 + \frac{8453}{13.27} I_{str} + 2311\sqrt{0.182 + \frac{A_{str}}{13.3}}$$

Let $I_{str} = 2.424 + 1.877x$

$A_{str} = 0.969 + 0.5x$

Therefore

$$2416 \leq 46.49 + 637(2.424 + 1.877x) + 2311\sqrt{0.25 + 0.037x}$$

The solution for x from the inequality is

$$x \geq -0.256 \text{ in.}$$

Therefore

$$I_4 = 1.94 \text{ in}^4$$

$$A_4 = 0.84 \text{ in}^2$$

Floor 3:

If $r_o = 186$ inches, $N_{app} = 1964$ pounds per inch, and $u_3 = 15.6$ inches, then

$$1917.5 \leq 541.9 I_{str} + 2311\sqrt{0.25 + 0.037x}$$

$$1917.5 \leq 1313.5 + 1017x + 2311\sqrt{0.25 + 0.037x}$$

The solution for x from the inequality is

$$x \geq 0.498 \text{ in.}$$

Therefore

$$I_3 = 1.48 \text{ in}^4$$

$$A_3 = 0.72 \text{ in}^2$$

Floor 2:

If r_o = 186 inches, N_{app} = 1442 pounds per inch, and u_2 = 22 inches, then

$$1395.5 \leq 384I_{str} + 2311\sqrt{0.182 + \frac{A_{str}}{22}}$$

$$1395.5 \leq 384(2.424 + 1.8769x) + 2311\sqrt{0.226 + 0.023x}$$

The solution for x from the inequality is

$$x \geq 0.81 \text{ in.}$$

Therefore

$$I_2 = 0.90 \text{ in}^4$$

$$A_2 = 0.56 \text{ in}^2$$

No stringers are required for floor 1.

The results of the computation for the stringer cross sections and the weights of the stringers are presented in table XI. The weight of the pressure skin is

$$W_{skin} = 2\pi(186)(0.182) \times 5(108)(0.1)$$

$$W_{skin} = 11\ 479 \text{ lb}$$

The total weight of the primary external LQM 2 structure (pressure-skin weight plus stringer weight) is 14 343 pounds.

5.0 FLOORING

5.1 GENERAL

The flooring must be designed to withstand equipment loadings that exist at launch. The loadings that exist during operational orbit conditions are insignificant when compared with the maximum launch loads. The design selected for the flooring is an aluminum honeycomb sandwich structure supported by a network of high-strength lightweight beams. Because each floor is radiused about the space-base spin axis, a radial-beam-type support structure would be impractical. The more practical approach is the use of curved beams that have the appropriate radii of curvature and that are oriented to run in the plane of the floor curvature. This type of support structure is used for this analysis. Because the ratio of the beam depth to the radius of curvature is considerably less than 10, the beams are assumed to be straight for the beam stress analysis. The error is slight if the radius of curvature is more than 10 times the depth of the beam (ref. 8). The floors are designed to withstand a uniform loading of 1.72 lb/in^2 (slightly less than 250 lb/ft^2), which is consistent with 30 000 pounds distributed uniformly over a 725 ft^2 area in a 5g launch environment. The high-strength beams allow a redistribution of loading such that concentrated loadings can be present and can be put directly into the beams.

The method of analysis includes the examination of various beam spacings and the selection of the optimum combination of beams and honeycomb sandwich structure that spans the beams. Because intercostal beams are being considered for concentrated loadings, a practical limit of 52 inches is set for the spacing distance. Beginning with 36-inch spacing, beam spacing in 4-inch increments is examined.

5.2 METHOD OF CALCULATION

5.2.1 Beams

The analysis is based on straight-beam theory, although a slight radius of curvature exists. The beams, made from a titanium alloy that has a tensile-yield strength of 150 000 psi and a shear strength of 90 000 psi, are assumed to have fixed end conditions to minimize floor deflection at launch. Deflection checks were made, but only excessive

deflection will affect the beam design. The following equations and formulas are used for the beam analysis.

$$M_{max.} = \frac{wl^2}{12}$$

$$V_{max.} = \frac{wl}{2}$$

$$\sigma = \frac{M}{S}$$

$$\tau = \frac{V}{A}$$

$$\delta_{max.} = \frac{wl^3}{384EI}$$

$$W = (n)(l)(A)(\rho)$$

$$w = pu$$

The beam length l and the number of beams n are determined graphically. The beams cannot abut the circumference of the outer-wall circle because of attachment fittings; therefore, a precise trigonometric determination of the length is unnecessary. Also, when the beam spacing is varied, a graphical determination minimizes the effort required to approximate the beam lengths. The beams are positioned symmetrically about the center of the floor, thus accounting for the factor n.

5.2.2 Honeycomb Sandwich Structure

The formulas and equations for the analysis of the honeycomb sandwich structure are found in reference 9. It is assumed that the sandwich paneling is rectangular and fixed at all edges. The face-sheet thickness is chosen arbitrarily as 0.020 inch, which appears to be a practical size for a floor surface that must withstand traffic, impacts from dropped equipment, and so forth. The face sheets are constructed of aluminum with a tensile-yield strength of 30 000 psi. The core is aluminum that has a density of 4.5 lb/ft^3, a shear strength of 205 psi, and a shear modulus of elasticity G_c of 25 600 psi. The ratio of side lengths is assumed to be that which gives a close approximation

for the selection of plate parameters for maximum bending moment and shear load. The maximum bending moments and shear loads are determined from standard isotropic plate theory (ref. 10), and these load values are used in the sandwich-structure equations. The following equations apply.

$$M_{max.} = \beta w d^2$$

$$V_{max.} = \alpha w d$$

$$\sigma_f = \frac{E_f z M}{B}$$

$$\tau_c = \frac{V}{t_c + t_f}$$

$$z = \frac{t_c}{2} + t_f$$

$$B = \frac{1}{2} E_f F \left(t_c + t_f\right)^2$$

$$\delta = \frac{w d^4}{384 D} + \frac{w d^2}{8 S'}$$

$$D = \frac{B}{1 - \nu^2}$$

$$S' = \frac{\left(t_c + t_f\right)^2}{t_c} G_c$$

5.3 CALCULATIONS

5.3.1 Beams

The calculations are omitted, but the results of the beam-spacing analysis are presented in table XII. The section modulus is determined, and a beam with the approximate section modulus required is selected

from tabulated beam data (ref. 7). Then, the corresponding inertia and area are used from the existing data. By using this technique, the time required for calculation is saved with only a slight sacrifice in optimization.

5.3.2 Honeycomb Sandwich Structure

The detailed mathematical calculations are omitted. The results of the analysis are given in table XIII.

5.4 SUMMARY

The combined weights of the beams and the honeycomb sandwich structure are given in table XIV. Based on combined weight, a 48-inch beam spacing, which gives a total weight of approximately 1700 pounds, is chosen. The general geometrical layout of the beam network that is positioned symmetrically about the tunnel is shown in figure 7.

6.0 COMPUTATION OF TUNNEL THICKNESS AND TUNNEL WEIGHT

6.1 TUNNEL THICKNESS AND TUNNEL WEIGHT OF LQM 1

The tunnel must withstand a 14.65-psi pressure differential (internal or external) and the tension loads induced by the end bulkheads. The tunnel wall thickness that will meet these requirements is computed as follows.

6.1.1 External Pressure Differential

A wall thickness is required such that no buckling in the skin occurs as a result of the external pressure differential. Given a pressure limit of 14.65 psi, a safety factor of 2, a pressure design of 29.30 psi, and using the equation

$$p = \frac{0.807Et^2}{l'r_i}\sqrt[4]{\left(\frac{1}{1-\nu^2}\right)^3\frac{t^2}{r_i^2}}$$

the computation is completed as follows. If $r_i = 36$ inches, $l' = 108$ inches, $E = 1 \times 10^7$ psi, and $\nu = 0.3$, then

$$29.2 \le \frac{0.807\left(10^7\right)t^2}{(108)36}\sqrt[4]{\left[\frac{1}{1-(0.3)^2}\right]^3\frac{t^2}{(36)^2}}$$

$$29.2 \le 2070t^2\,\frac{1.08}{6}\,\sqrt{t}$$

$$29.2 \le 370t^2\,\sqrt{t}$$

$$t^2 \ge \frac{0.059}{\sqrt{t}}$$

$$t \geq \frac{0.24}{\sqrt[4]{t}}$$

$$t \geq 0.320 \text{ in.} \tag{5}$$

A wall thickness of 0.320 inch is needed to prevent buckling caused by an external pressure differential of 14.65 psi.

6.1.2 Internal Pressure and End-Bulkhead Loads

A wall thickness is required such that stress failure in the hoop direction does not occur. Given a pressure limit of 14.65 psi, a safety factor of 1.5, a pressure design of 21.9 psi, and using a hoop stress equation, the wall thickness is computed as follows.

$$\sigma_\theta = \frac{pr_i}{t} = \frac{(21.9)36}{t}$$

$$\frac{788}{t} \leq 30\ 000 \text{ psi}$$

$$t \geq 0.000026 \text{ in.} \tag{6}$$

The longitudinal stress is caused by internal pressure and by the loads induced by the end bulkheads. A wall thickness is required such that stress failure in the longitudinal direction does not occur. The wall thickness is computed as follows.

$$\sigma_l = \frac{pr}{2t} + \frac{N_i}{t}$$

From section 4.1.2

$$N_i = \frac{2r_i + r_o}{r_i}\left[(r_o - r_i)\frac{p}{6}\right]$$

$$N_i = \frac{2(36) + 186}{36} \left(150 \frac{p}{6}\right)$$

$$N_i = 179p$$

$$\sigma_1 = p \frac{18}{t} + \frac{179p}{t} = \frac{197p}{t}$$

The σ_1 should be less than σ_y. Therefore

$$\frac{197p}{t} \leq 30\ 000 \Rightarrow t \geq \frac{4314.3}{30\ 000}$$

$$t \geq 0.144 \text{ in.} \qquad (7)$$

The only thickness that will satisfy inequalities (5), (6), and (7) for t is $t \geq 0.320$ inch. By using 0.320 inch for the tunnel thickness, the weight of the LQM 1 tunnel is given by

$$W = 2\pi r_i t \rho (L) = 2\pi(36)(0.320)(0.1)(1152)$$

$$W = 8334 \text{ lb}$$

6.2 TUNNEL THICKNESS AND TUNNEL WEIGHT OF LQM 2

The tunnel thickness of LQM 2 is the same as that of LQM 1, but the length is different. The tunnel weight of LQM 2 is calculated as follows.

$$W = 2\pi r_i t \rho (L) = 2\pi(36)(0.32)(0.1)(5)(108)$$

$$W = 3906 \text{ lb}$$

7.0 END BULKHEADS

7.1 GENERAL

The end bulkheads are used to close off the ends of the main space-base modules to allow for pressurization. Although the ideal configuration incorporates the lightest weight bulkhead capable of doing the job, this design usually is unacceptable because of the relatively large space requirements. For example, either a hemispherical shell or a slightly ellipsoidal shell is the most likely candidate for an end closure on the outboard and inboard ends of LQM 2 and on the outboard end of LQM 1. The use of a hemispherical shell results in the addition of 15.5 feet to each of the ends; the use of an ellipsoidal shell results in the addition of approximately 11 feet to each end. Decreasing the semiminor axis of the ellipsoid to save space requires the addition of a reinforcement ring to compensate for compressive hoop stresses and adverse deflections. The resulting weight increase depends on the size and strength of ring required.

The optimum space-saving design is a flat-plate type of design wherein the shell is a network of beams with an appropriate covering. This configuration results in large weight penalties. Even if the outboard bulkhead for each LQM functions as the outboard floor, the approach is undesirable because of the amount of weight. Neither the ideal structural design nor the ideal minimum-space design is particularly satisfactory; consequently, some compromise between the two designs must be made.

Before settling on a design approach, the existing interface or boundary conditions must be examined. Establishing the correct conditions often creates problems; in this case, however, a solution to the problem is offered that allows a straightforward membrane analysis without requiring the use of excessive reinforcements. At the same time, the amount of added length is reduced to an acceptable value. Although the maximum allowable length to which the space-base modules can be extended has not been defined, the selected design is believed to be within the permissible envelope.

For the cylindrical body of LQM 2 with the 6-foot tunnel located axisymmetrically, the use of a semitoroidal shell connecting the tunnel to the cylinder wall at the inboard- and outboard-bulkhead locations appears to be an ideal design. A hemispherical or slightly ellipsoidal closing over the outboard end of the tunnel would complete the outboard bulkhead, and a relatively flat hatch inside the tunnel at the inboard-bulkhead location would complete the LQM 2 pressure vessel. The hatch

would be a temporary removable closure that would be used only during launch and as an emergency closure during operation.

The same semitoroidal shell at the outboard-bulkhead location and the same type of temporary hatch proposed for LQM 2 are required for LQM 1. A different approach is required for the inboard-bulkhead location of LQM 1. Because the bulkhead at this location acts as the restraint for the tunnel, the bulkhead must put a loading into the tunnel equal to the loading put into the tunnel at the outboard station of LQM 2. The loadings at the outboard bulkhead of LQM 1 and at the inboard bulkhead of LQM 2 effectively cancel each other and, therefore, make no contribution to reacting the tension load in the tunnel. In the operational mode, a pressure differential across the inboard bulkhead of LQM 1 does not exist. This condition precludes the use of pressure to counteract the tunnel loading; the pressure must be reacted by the bulkhead itself. In addition, the inboard bulkhead must be capable of reacting pressure from either side because LQM 1 possibly may lose pressure while the hub and the tunnel leading to LQM 2 remain pressurized. The discussion of the inboard bulkhead is defined further in section 7.4. To complete the pressure-holding requirements of LQM 1, the tunnel has a temporary hatch at the inboard-bulkhead location similar to the hatches previously mentioned.

Because the scope of this particular analysis does not include the design of windows, doors, hatches, and so forth, the three temporary hatches that close the tunnel at the various locations are not considered in this section. The analysis includes semitoroidal shells, the inboard bulkhead of LQM 1, and the tunnel end closure on the outboard location of LQM 2.

7.2 SEMITOROIDAL PRESSURE SHELL

7.2.1 General

The goal is to design minimum-weight end bulkheads that require a minimum amount of space. The weight and space parameters can be met by using the semitoroidal shell with an elliptical cross section. Determination of the exact amount of ellipticity that can be tolerated and the resulting stresses is the objective of this analysis.

7.2.2 Equation Derivation

The design and nomenclature to support the analysis are shown in figures 8, 9, and 10. The toroidal shell is formed by the revolution of a semiellipse with the major diameter 2a and minor diameter 2b around

an axis with a radius r. The analysis examines the portion of the shell designated A-A-B-B (fig. 8) so that the only membrane forces at B-B are horizontal, and the vertical components of the membrane forces exist only at A-A. The positive values of the variable x' are from the center of the ellipse outward, and the positive values of the variable y' are from the center of the ellipse upward.

The equation of ellipse is

$$\frac{(x')^2}{a^2} + \frac{(y')^2}{b^2} = 1 \tag{8}$$

The equation of equilibrium from figures 8 and 9 is

$$\Sigma F_v = 0$$

$$2\pi r_o N_\phi \sin \phi = p\pi\left(r_o^2 - r_T^2\right)$$

$$r_o = r_T + x'$$

$$r_o^2 = r_T^2 + 2r_T x' + (x')^2$$

$$2\left(r_T + x'\right)\sin \phi N_\phi = p\left[(x')^2 + 2r_T x'\right] \tag{9}$$

From figure 9

$$\sin \phi = \frac{-dy'}{\left[(dy')^2 + (dx')^2\right]^{1/2}}$$

$$\sin \phi = \frac{-\frac{dy'}{dx'}}{\left[1 + \left(\frac{dy'}{dx'}\right)^2\right]^{1/2}} \tag{10}$$

From equation (8)

$$(y')^2 = b^2\left[1 - \frac{(x')^2}{a^2}\right]$$

$$y' = \pm b\left[1 - \frac{(x')^2}{a^2}\right]^{1/2}$$

where y' is positive for the upper half of the ellipse. Then

$$\frac{dy'}{dx'} = b\left(\frac{1}{2}\right)\left[1 - \frac{(x')^2}{a^2}\right]^{-1/2}\left(-\frac{2x'}{a^2}\right)$$

$$\frac{dy'}{dx'} = -\frac{bx'}{a\left[a^2 - (x')^2\right]^{1/2}} \tag{11}$$

Substituting equation (11) into equation (10)

$$\sin \phi = \frac{bx'}{a\left[a^2 - (x')^2\right]^{1/2}\left\{1 + \frac{b^2(x')^2}{a^2\left[a^2 - (x')^2\right]}\right\}^{1/2}}$$

$$\sin \phi = \frac{bx'}{\left[a^4 - a^2(x')^2 + b^2(x')^2\right]^{1/2}} \tag{12}$$

Substituting equation (12) into equation (9)

$$\frac{2\left(r_T + x'\right)bx'}{\left[a^4 - a^2(x')^2 + b^2(x')^2\right]^{1/2}} N_\phi = p\left[(x')^2 + 2r_T x'\right]$$

$$N_\phi = \frac{p\left(2r_T + x'\right)\left[a^4 - a^2(x')^2 + b^2(x')^2\right]^{1/2}}{2b\left(r_T + x'\right)} \tag{13}$$

Equation (13) is the expression for the meridional forces (pounds per length) and is in agreement with reference 11.

From reference 10

$$\frac{N_\phi}{r_\phi} + \frac{N_\theta}{r_\theta} = p \tag{14}$$

From reference 12

$$r_\phi = a^2 b^2 \left[\frac{(x')^2}{a^4} + \frac{(y')^2}{b^4}\right]^{3/2} \tag{15}$$

From equation (8)

$$(y')^2 = \frac{b^2}{a^2}\left[a^2 - (x')^2\right]$$

$$r_\phi = a^2b^2\left\{\frac{(x')^2}{a^4} + \frac{b^2\left[a^2 - (x')^2\right]}{a^2b^2}\right\}^{3/2}$$

$$r_\phi = \frac{\left\{a^4 - \left[a^2(x')^2 + b^2(x')^2\right]\right\}^{3/2}}{a^4b} \tag{16}$$

From figure 9

$$r_\theta = \frac{r_o}{\sin\phi}$$

$$r_o = r_T + x'$$

Using equation (12)

$$r_\theta = \frac{\left(r_T + x'\right)\left[a^4 - a^2(x')^2 + b^2(x')^2\right]^{1/2}}{bx'} \tag{17}$$

Substituting equations (17), (16), and (13) into equation (14)

$$p = \frac{p(2r_T + x')\left[a^4 - (x')^2(a^2 - b^2)\right]^{1/2} a^4 b}{2b(r_T + x')\left[a^4 - (x')^2(a^2 - b^2)\right]^{3/2}}$$

$$+ \frac{N_\theta b x'}{(r_T + x')\left[a^4 - (x')^2(a^2 - b^2)\right]^{1/2}}$$

$$N_\theta = \frac{p(r_T + x')\left[a^4 - (x')^2(a^2 - b^2)\right]^{1/2}}{bx'}$$

$$- \frac{p\left[a^4 - (x')^2(a^2 - b^2)\right]^{-1/2}(2r_T + x')a^4}{2bx'}$$

$$N_\theta = \frac{p}{2bx'}\Big\{2(r_T + x')\left[a^4 - (x')^2(a^2 - b^2)\right]^{1/2}$$

$$- a^4(2r_T + x')\left[a^4 - (x')^2(a^2 - b^2)\right]^{-1/2}\Big\}$$

$$N_\theta = \frac{2p(r_T + x')\left[a^4 - (x')^2(a^2 - b^2)\right] - pa^4(2r_T + x')}{2bx'\left[a^4 - (x')^2(a^2 - b^2)\right]^{1/2}} \qquad (18a)$$

Reducing equation (18a)

$$N_\theta = \frac{p(x')^2\left(b^2 - a^2\right) + pr_T x'\left(b^2 - a^2\right) + \frac{pa^4}{2}}{b\left[a^4 + (x')^2\left(b^2 - a^2\right)\right]^{1/2}} \tag{18b}$$

The expression for the hoop forces N_θ is in agreement with reference 11.

The term $[a^4 - (x')^2(a^2 - b^2)]$ is always positive because the maximum value of $(x')^2$ is a^2 and, therefore, the minimum value of the bracketed term is a^2b^2. The maximum value of the bracketed term (at $x' = 0$) is a^4. Therefore, N_ϕ is always positive because $2r_T + x'$ and $r_T + x'$ are always positive $(r_T > x')$. The meridional stresses are greater than the hoop stresses, and, therefore, dictate the shell thickness. This hoop stress maximum value is at $x' = -a$. For the hoop force N_θ, all of the individual terms are positive; consequently, hoop stresses can become compressive only if the numerator of equation (18a) is negative; that is, if

$$a^4\left(2r_T + x'\right) > 2p\left(r_T + x'\right)\left[a^4 - (x')^2\left(a^2 - b^2\right)\right]$$

The minimum allowable value of b is that obtained when the hoop force reaches zero. From equation (18a), N_θ is minimum at $x' = +a$. Therefore, substituting $x' = +a$ in the previous inequality, the minimum value of b can be determined by changing the inequality to an equality.

$$a^4\left(2r_T + a\right) = 2\left(r_T + a\right)\left(a^2b^2\right)$$

Therefore

$$b^2 = a^2 \frac{\left(2r_T + a\right)}{2\left(r_T + a\right)}$$

and

$$\frac{b}{a_{min.}} = \sqrt{\frac{\left(2r_T + a\right)}{2\left(r_T + a\right)}} \tag{19}$$

The formula for the length of the perimeter of an ellipse (ref. 12) is

$$P = \pi(a + b)k \tag{20}$$

where $k = \left(1 + \frac{1}{4} m^2 + \frac{1}{64} m^4 + \frac{1}{256} m^6 + \ldots\right)$ and $m = \frac{a - b}{a + b}$.

The approximate area of the semitoroidal cross section of thickness t is

$$A = \frac{1}{2} Pt \tag{21}$$

The approximate volume of the semitoroidal shell material is

$$\text{volume} = 2\pi r_T(A) = \pi r_T Pt \tag{22}$$

and the weight is

$$W = \rho(\text{volume}) = \rho\pi r_T Pt \tag{23}$$

7.2.3 Calculations

Given

$$p = (14.65)(144)\ \text{lb/ft}^2$$

$$a = 6.25\ \text{ft}$$

$$r_T = 9.25\ \text{ft}$$

$$\sigma_y = 30\ 000\ \text{psi}$$

$$fs = 1.5$$

$$sf = 1.25$$

From equation (19)

$$b = 6.25\left[\frac{(2)(9.25) + 6.25}{2(9.25 + 6.25)}\right]^{1/2}$$

$$b = (6.25)(0.894)$$

$$b = 5.58\ \text{ft}$$

To determine the maximum meridional stress

$$\sigma_\phi = \frac{N_\phi}{t} = \sigma_y$$

From equation (13), setting $x' = -a$ yields

$$N_\phi = \frac{(14.65)(144)[(2)(9.25) - 6.25](5.58)(6.25)}{2(5.58)(9.25 - 6.25)}$$

$$N_\phi = 27\ 011 \text{ lb/ft}$$

$$t = \frac{N_\phi (fs)(sf)}{\sigma_y} = \frac{27\ 011(1.5)(1.25)}{(30\ 000)(12)}$$

$$t = 0.141 \text{ in.}$$

To determine weight

$$m = \frac{a - b}{a + b} = 0.056635$$

Therefore

$$k \approx 1.001$$

$$P = \pi(6.25 + 5.58)(1.001)$$

$$P = 37.202 \text{ ft}$$

For $\rho = 0.1 \text{ lb/in}^3$ and from equation (23)

$$W = (0.1)(\pi)(9.25)(12)(37.202)(12)(0.14)$$

$$W = 2180 \text{ lb}$$

7.3 TUNNEL END CLOSURE

7.3.1 General

Analyses of spherical and elliptical pressure closures are available from many sources. The maximum meridional forces for either spherical or elliptical pressure closures are the same because the forces equal the projected area multiplied by the pressure and divided by the perimeter. However, the elliptical pressure closure develops compressive hoop stresses if the square of the semimajor axis exceeds twice the square of the semiminor axis (ref. 10).

The choice between the hemispherical or elliptical closure should be based on weight and space. The elliptical closure weighs slightly less than the hemispherical closure. The consideration of space in this analysis is opposite that used for the semitoroidal shell. Because the semitoroidal shell extends the end of the structure approximately 5.5 feet, the closure of the tunnel can be accomplished by any means as long as the extension of 5.5 feet is not exceeded. Actually, maximum space, which would allow for incorporation of elevator mechanisms or other functional equipment, may be desirable. Because of the previously mentioned considerations and because the analysis is straightforward, the calculations for both the hemispherical and elliptical closures are presented, leaving the choice of the type of closure to be made at a later date.

7.3.2 Calculations

7.3.2.1 Hemispherical closure.- From reference 10

$$N_\theta = N_\phi = \frac{pa}{2}$$

$$\sigma_y = 30\ 000$$

$$fs = 1.5$$

$$sf = 1.25$$

$$a = 3.0 \text{ ft}$$

$$p = 14.65 \text{ psi}$$

$$N_\phi = \frac{(14.65)(3.0)(12)}{2} = 265 \text{ lb/in.}$$

$$t = \frac{N_\phi (fs)(sf)}{\sigma_y}$$

$$t = \frac{(265)(1.5)(1.25)}{30\ 000}$$

$$t = 0.017 \text{ in.}$$

This thickness is insufficient to be practical. Because the closure will be welded, handled during assembly, and so forth, the thickness is increased arbitrarily to 0.10 inch.

$$W = A_s t\rho = 2(\pi r^2)t\rho$$

For $\rho = 0.1$ lb/in^3

$$W = 2(\pi)(9)(144)(0.10)(0.1)$$

$$W = 81 \text{ lb}$$

7.3.2.2 Elliptical closure.- Because the maximum meridional forces will be the same for the elliptical closure as for the hemispherical closure, the thickness will be the same (t = 0.10). If a = 3 feet and $a^2 > 2b^2$, then

$$b_{min.} = \frac{a}{\sqrt{2}} = 0.707a$$

$$b_{min.} = 2.1 \text{ ft}$$

The approximate surface area for an ellipsoid of these dimensions is 45.7 ft^2. Therefore, the weight is

$$W = A_s t \rho$$

For $\rho = 0.1$ lb/in^3

$$W = (45.7)(144)(0.10)(0.1)$$

$$W = 66 \text{ lb}$$

7.3.3 Summary

The 81-pound hemispherical closure adds 3 feet of length that would be available for the incorporation of functional equipment. Although the lighter 66-pound ellipsoidal closure has a weight advantage, the 2.1 feet of added length offers less space for equipment.

7.4 INBOARD BULKHEAD FOR LQM 1

7.4.1 General

The purposes of the inboard-bulkhead closure are (1) to function as a pressure wall for pressure acting from either direction and (2) to serve as a device to react the tunnel loading that originates from the inner perimeter of the semitoroidal shell and tunnel closure that are located on the outboard end of LQM 2. These loads total approximately 570 000 pounds and must be reacted in some manner by the inboard bulkhead of LQM 1. In general, the reasoning used in choosing a toroidal shell for the other pressure closures also applies to the inboard-bulkhead closure; however, a toroidal shell alone cannot withstand the tunnel loading. Also, because the closure area is significantly smaller than that of the other closures, a flat-plate type of closure may be a competitive design.

An additional structure such as tension rods or shear webs may be required to react the tunnel loading. A partial toroidal shell with a cross-sectional radius of curvature equal to that of the larger toroid at the outboard end of LQM 1 is another means by which the tunnel loading can be counteracted. This type of shell would be tangent to the

tunnel. The shell would react the tunnel loading equally; however, a reinforcing ring at the outer wall would be required to take the radial component of the interface load because the shell would not be tangent at the outer wall.

Several configurations were examined before a conclusion concerning the type of bulkhead to be used was reached.

a. Toroidal shell with tension rods

b. Flat plate with tension rods

c. Toroidal shell with shear webs

d. Flat plate with shear webs

e. Conical shell

f. A partial toroidal shell which has a cross-sectional radius of curvature equal to that of the larger toroidal shell

The general design of each of these configurations is depicted in figures 11 to 16, respectively. The following analyses examine the requirements for using tension rods and shear webs to react tunnel loading. These requirements are combined with the requirements for the toroidal shell and the flat-plate type of pressure barrier, resulting in four workable systems. The four systems, then, are compared with the fifth approach (which incorporates a conical-frustrum structure to function as a pressure barrier and to react tunnel rods) and to the sixth approach that incorporates the partial toroidal closure. A choice of bulkhead is made by using weight as the primary factor for evaluation.

7.4.2 Tension Rods

7.4.2.1 General.- Two variables must be considered when tension rods are analyzed. First, the number of rods to be used is considered; second, the angle at which these rods should be positioned is determined. The rods are pinned to structural rings that are located on the outer wall and on the tunnel. The loading into the ring improves with the increase in the number of rods used. However, the number of rods is limited because enough space must be left between rods to allow a man to pass. Because of this limitation, 10 rods were used. Approximately 10 square feet of passage area is available with this configuration. The following analysis provides suitable data for the selection of the angle at which the rods should be positioned.

7.4.2.2 Analysis.- From figure 17, if nF_v = tunnel loading (30 191 lb/ft), then

$$nF_v = 30\ 191(6\pi)\ \text{lb} \tag{24}$$

and

$$\Sigma M_g = 0 = F_v l \sin\theta - F_h l \cos\theta$$

$$F_h = F_v \tan\theta$$

$$F_h = \frac{(30\ 191)(6\pi)\tan\theta}{n} \tag{25}$$

If titanium rods with a yield strength of 150 000 psi are used, then

$$\sigma_y = \frac{F}{A}(fs)$$

$$F^2 = F_v^2 + F_h^2 = \frac{(30\ 191)^2(6\pi)^2}{n^2} + \frac{(30\ 191)^2(6\pi)^2\tan^2\theta}{n^2}$$

$$F = \frac{(30\ 191)(6\pi)}{n}\left(1 + \tan^2\theta\right)^{1/2} \tag{26}$$

$$F = \frac{A\sigma_y}{fs} = 100\ 000A$$

$$100\ 000A = \frac{(30\ 191)(6\pi)}{n}\left(\frac{1}{\cos\theta}\right)$$

$$A = \frac{(3.0191)(0.6)(\pi)}{n\cos\theta} \tag{27}$$

The expression for the total weight of the tension rods is

$$W = nAl\rho \tag{28}$$

If $l = 2a/\sin\theta$, then

$$W = \frac{nA\rho(2a)}{\sin\theta}$$

$$W = \frac{(3.0191)(0.6)(\pi)}{\cos\theta}\,\frac{(\rho)(2a)}{\sin\theta} \tag{29}$$

From figure 17, the expression for the extended length e below the outer ring is

$$e = l\cos\theta$$

If

$$2a = 42 \text{ in.}$$

$$e = \frac{42\cos\theta}{\sin\theta} \tag{30}$$

For the weight to be minimized, $\sin\theta\cos\theta$ must be a maximum value. By differentiating this expression with respect to θ and setting it equal to zero, the value of θ that makes $\sin\theta\cos\theta$ a maximum can be determined.

$$\frac{d(\sin\theta\cos\theta)}{d\theta} = 0$$

$$(\sin\theta)(-\sin\theta) + (\cos\theta)(\cos\theta) = 0$$

$$\sin^2\theta = \cos^2\theta$$

$$\sin\theta = \cos\theta$$

$$\theta = 45^\circ$$

The rod angle of 45° will result in unnecessarily high radial loads into the outer ring. The radial loads can be decreased by decreasing the rod angle, but higher rod weight results. In LQM 1, the interface of the 15-foot-diameter cylindrical section and the conical frustrum appears to be the best practical position for the attachment of the rods to the tunnel. By positioning the rods at this interface, a rod angle of approximately 7° is achieved.

The data presented in table XV are the results of equations (25), (29), and (30). It is anticipated that by reducing the magnitude of the radial component of rod loading into the rings, the weight saving that results would be greater than the increase in rod weight. Therefore, a 7° rod angle is used to choose a rod design.

7.4.3 Shear Webs

7.4.3.1 General.- Many methods exist by which shear webs can be used to react tunnel loading. The volume in which these webs will be located can be used for material storage or tankage (water, for example). This use necessitates a shear-web pattern that would allow reasonable designs for tankage or shelving. Also, adequate room for stairway passage must be available. Because the primary design stress will be from bending, the cross-sectional moment of inertia should be comparatively large. This criterion is suggestive that having several sets of webs, each of which has a high moment of inertia in proportion to the height, would be desirable. An arrangement of shear webs spaced so that toroidal tanks could be placed between the webs is possible.

The shear-web interface with the wall structure also must be evaluated. The webs will be putting shear force and large moments into the wall. The wall, which is primarily a pressure vessel, should be reinforced locally to prevent buckling or localized failure. The shear web interface with the wall structure will be considered only if the shear-web approach becomes a competitive design. For initial comparison, only the shear webs are analyzed.

A rigorous analysis would be required to examine all of the variables that are possible during optimization of this design. For this reason, a somewhat arbitrary establishment of certain parameters is made to facilitate the analysis. First, the number of shear webs is considered. It appears logical to place three sets of four shear webs (12 webs) 90° apart. Second, it is established that the webs are I-bea with an 0.25-inch flange thickness, an 0.25-inch web thickness, and a 6-inch flange width. The maximum allowable deflection of the webs is 0.01 inch. The following analysis determines the physical requirements of the shear webs if the webs are fixed at the outer wall. The total weight is based on the previously mentioned assumed parameters and is used for comparison with the tension rod weights.

7.4.3.2 Analysis.- The shear-web configuration is shown in figure 18. Because the shear webs are fixed to the tunnel and deflecte down, the slope at point g is zero. Combining appropriate examples from reference 18, the following equations apply.

$$\frac{\frac{1}{2}\left(\frac{F}{n}\right)(l)^2}{EI} = \frac{M_g l}{EI}$$

$$M_g = \frac{1}{2}\left(\frac{F}{n}\right)(l) \tag{31}$$

$$M_{max.} = M_g = M_{g'} = \frac{1}{2}\left(\frac{F}{n}\right)(l)$$

$$V_{max.} = \frac{F}{n}$$

$$\sigma_{max.} = \frac{M_{max.}\left(\frac{h}{2}\right)}{I} \tag{32}$$

$$\tau_{max.} = \frac{V_{max.}}{A} \tag{33}$$

The deflection is

$$\delta_g = \frac{\frac{1}{3}\left(\frac{F}{n}\right)(1)^3}{EI} - \frac{1}{2}\frac{M_g 1^2}{EI} \tag{34}$$

$$\delta_g = \frac{\left(\frac{F}{n}\right)(1)^3}{3EI} - \frac{\left(\frac{F}{n}\right)(1)^3}{4EI}$$

$$\delta_g = \frac{1}{12}\frac{\left(\frac{F}{n}\right)(1)^3}{EI} \tag{35}$$

From the assumption that $\delta_{g,max.} = 0.01$

$$0.01 = \frac{1}{12}\frac{\left(\frac{F}{n}\right)(1)^3}{EI}$$

$$\frac{\left(\frac{F}{n}\right)}{I} = \frac{0.01(12)(E)}{1^3} \tag{36}$$

Assuming $n = 12$ and if

$$1 = 42$$

$$F = 570\ 000 \text{ lb}$$

$$E = 10.5(10)^6 \text{ psi}$$

then

$$I = \frac{570\ 000(42)^3}{(12)(0.01)(12)(10.5)(10)^6}$$

$$I = 1393\ \text{in}^4$$

The following calculations were performed to determine the shear-web cross section (fig. 19).

$$I = \frac{t(h)^3}{12} + \frac{2(d)(t)^3}{12} + 2dt\left(\frac{h}{2} + \frac{t}{2}\right)^2 \tag{37}$$

$$A = 2(dt) + ht = t(2d + h) \tag{38}$$

Substituting $t = 0.25$ inch and $d = 6.0$ inches in equation (37)

$$1393 = \frac{(0.25)h^3}{12} + \frac{2(6.0)(0.25)^3}{12} + \frac{2(6)(0.25)}{4}(h + 0.25)^2$$

$$1393 = \frac{h^3}{48} + \frac{1}{64} + \frac{3}{4}\left(h^2 + \frac{h}{2} + \frac{1}{16}\right)$$

$$1393 = \frac{h^3}{48} + \frac{1}{64} + \frac{3}{4}h^2 + \frac{3}{8}h + \frac{3}{64}$$

$$\frac{h^3}{48} + \frac{3}{4}h^2 + \frac{3}{8}h + \frac{1}{16} - 1393 = 0$$

$$h^3 + 36h^2 + 18h - 66\ 861 = 0$$

Solving for h yields

$$h = 31.3 \text{ in.}$$

From equation (38)

$$A = (0.25)[(2 \times 6) + 31.3] = 10.825 \text{ in}^2$$

The weight per web equals $Al\rho$; therefore

$$W = (10.825)(42)(0.1) = 45.465 \text{ lb}$$

For 12 beams, the weight is 545.58 pounds.

7.4.3.3 Summary.- Although the total weight of the shear webs is based on a somewhat arbitrary selection of parameters, it appears that enough weight saving is obtained by the 7° tension rod to discontinue further shear-web evaluation. If the weight saving alone does not justify the elimination of the shear-web approach, then the complexity of securing the webs to the outer wall and the subsequent weight increase that results with the increased structure is enough to discourage shear-web use.

7.4.4 Toroidal Bulkhead

7.4.4.1 General.- The pressure bulkhead must sustain the pressure from either direction. With a semitoroidal shell, only tensile membrane stresses will result with internal pressure; compressive buckling-type stresses will result when the pressure is reversed. If a complete toroidal shell were internally pressurized to the operating pressure, the shell would experience only tensile stresses. However, the weight of the complete toroidal shell is twice that of a semitoroidal shell, which experiences only tension. On the other hand, a semitoroidal shell capable of withstanding external pressure will require an increase in thickness that increases the weight accordingly. The analysis determines the increase in thickness required to prevent buckling of a semitoroidal shell. Then, the weights of the semitoroidal shell and the complete toroidal shell are compared.

7.4.4.2 Semitoroid.- An 0.23-inch shell thickness is required for an externally pressurized toroid (ref. 13). This thickness is based on a critical pressure of 29.4 psi (minimum). Curves based on two parameters (with the thickness as a variable) are used to determine thickness. This set of curves generally is used for analyses in which the thickness is known and the critical pressure can be found directly. Varying the thickness to obtain a given critical pressure requires an iterative process with interpolation which, while not exact, gives a good approximation of the minimum permissible thickness. This thickness is significantly larger than that required and compensates for the 20-percent scratch factor that would be added to the membrane stress thickness.

The weight of the semitoroidal shell is found by the use of equation (23) where $P = 2\pi a$.

$$W = \rho \pi r_T P t$$

$$W = \rho \pi r_T (2\pi a) t$$

$$W = (0.1)(\pi)(57)(2\pi)(24)(0.23)$$

$$W = 543 \text{ lb}$$

7.4.4.3 Full toroid.- Applying the analysis in section 7.2 to a circular cross section by setting $a = b$, the following calculations (using equation (13)) determine the required thickness of the full toroid.

$$N_\phi = \frac{p\left(2r_T + x'\right)\left[a^4 - a^2(x')^2 + b^2(x')^2\right]^{1/2}}{2b\left(r_T + x'\right)}$$

$$a = b$$

$$x' = -a(\text{point of maximum stress})$$

$$N_\phi = \frac{p(2r_T - a)(a^2)}{2a(r_T - a)}$$

$$N_\phi = \frac{pa(2r_T - a)}{2(r_T - a)} \tag{39}$$

This expression for maximum stress in a pressurized toroid with a circular cross section is the same as that contained in reference 8.

$$N_\phi = \frac{(14.65)(21)[(2)(57) - 21]}{2(57 - 21)}$$

$$N_\phi = 398.74 \text{ lb/in.}$$

If

$$\sigma_y = 30\ 000$$

$$fs = 1.5$$

$$sf = 1.25$$

$$t = \frac{x'_\phi(fs)(sf)}{\sigma_y}$$

then

$$t = \frac{(398.74)(1.5)(1.25)}{30\ 000}$$

$$t = 0.025 \text{ in.}$$

Because the thickness is too small to be practical, the thickness is increased to 0.10 inch. The weight of a full 0.10-inch-thick toroid is

$$W = A_s t\rho$$

where $A_s = 4\pi^2 a r_T$. Substituting the value for A_s

$$W = 4\pi^2 a r_T t\rho$$

$$W = 4(3.1416)^2(21)(57)(0.10)(0.1)$$

$$W = 473 \text{ lb}$$

7.4.4.4 Summary.- From the data presented, the conclusion can be drawn that the full toroid is the preferable choice. This is true especially when it is realized that the thickness of 0.10 inch is conservative. Because the factor governing shell thickness is the ability of the shell to be worked and welded, the thickness probably can be reduced to less than 0.10 inch.

The full toroid must be pressurized, a requirement that is unnecessary for the semitoroid. Thus, an operational or functional type of problem exists wherein the full toroid must not leak and must be monitored. If, in the final analysis, the toroidal closures are considered to be prime design candidates, these problems will be examined in detail.

7.4.5 Flat-Plate Bulkhead

7.4.5.1 General.- The more desirable pressure bulkhead is one in which the stresses are of the membrane type and in which minimum bending stresses are present. Such is the case with the toroidal shell previously discussed. The complexity of fabrication or volume requirements may dictate a flat-plate type of bulkhead in which the primary stresses are caused by bending. If the bulkhead is relatively small such that weight penalties are small with the flat plate, then it becomes necessary to consider an approach that is less than optimum.

The purpose for the inclusion of a flat-plate analysis is twofold. First, a possibility exists that a sandwich flat-plate bulkhead may be competitive; second, if requirements evolve for which a flat-plate bulkhead would be preferable, the analysis would be available.

7.4.5.2 Analysis.- The deflection at point O is taken to be zero, because the plate is fixed to the tunnel, which is assumed to have no vertical movement. Both solid and sandwich flat-plate bulkheads are analyzed.

7.4.5.2.1 Solid flat-plate bulkhead: The following formula (ref. 14 and fig. 20) applies.

$$\sigma_{max.} = \frac{\beta p a^2}{t^2} \tag{40}$$

where β is the plate parameter for bending, p is the applied pressure, and t is the thickness.

By interpolation, the value of β for the given plate geometry is 0.1834.

$$\sigma_{max.} = \frac{(0.1834)(14.65)(78)^2}{t^2}$$

$$\sigma_{max.} = \frac{\sigma_y}{fs} = \frac{30\ 000}{1.5} = 20\ 000 \text{ psi}$$

$$t^2 = \frac{(0.1834)(14.65)(78)^2}{20\ 000}$$

$$t = 0.91 \text{ in.}$$

$$W = \pi\left(r_o^2 - r_i^2\right)(t)(\rho) \tag{41}$$

$$W = \pi\left(78^2 - 36^2\right)(0.91)(0.1)$$

$$W = 1368 \text{ lb}$$

7.4.5.2.2 Sandwich flat-plate bulkhead: To analyze a sandwich flat-plate bulkhead, it is necessary to determine the maximum bending moment and shear loads in the plate. The loads are determined first from standard isotropic plate theory and then applied to formulas derived for sandwich flat-plate construction. The maximum bending moment and shear loads are developed in the analysis by the use of the approximate sandwich flat-plate construction equations. The correctness of the approach is suitable for the purposes of this report. The loadings are determined from the theory described in reference 10; reference 9 is used as a guideline for the sandwich flat-plate analysis.

For the development of moment and shear-load equations, the following equations apply (fig. 21).

$$\frac{d}{dr}\left[\frac{1}{r}\frac{d}{dr}\left(r\frac{d\delta}{dr}\right)\right] = \frac{Q}{D} \tag{42}$$

and

$$M_r = -D\left(\frac{d^2\delta}{dr^2} + \frac{\nu}{r}\frac{d\delta}{dr}\right) \tag{43}$$

where Q is the shear loading per unit length, δ is the deflection, and D is the flexural rigidity of the plate. By equilibrium considerations, the following equation can be written for the shear load as a function of the radius.

$$R_i(2\pi r_i) + Q(2\pi r) = p\pi\left(r^2 - r_i\right)$$

$$Q = \frac{p\left(r^2 - r_i^2\right)}{2r} - \frac{R_i r_i}{r} \tag{44}$$

From reference 14

$$R_i = \frac{\gamma' p r_o^2}{2\pi r_i} \tag{45}$$

By interpolation

$$\gamma' = 1.01$$

Then

$$R_i = \frac{(1.01)(14.65)(78)^2}{2\pi(36)}$$

$$R_i = 399 \text{ lb/in.}$$

From equation (42)

$$\frac{d}{dr}\left[\frac{1}{r}\frac{d}{dr}\left(r\frac{d\delta}{dr}\right)\right] = \frac{pr}{2D} - \frac{pr_i^2}{2rD} - \frac{R_i r_i}{rD}$$

Integrating once gives

$$\frac{d}{dr}\left(r\frac{d\delta}{dr}\right) = \frac{pr^3}{4D} - \frac{pr_i^2}{2D} r \ln r \frac{R_i r_i}{D} r \ln r + C_1' r$$

Integrating again gives

$$\frac{d\delta}{dr} = \frac{pr^3}{16D} - \frac{pr_i^2}{4D} r\left(\ln r - \frac{1}{2}\right) - \frac{R_i r_i}{2D} r\left(\ln r - \frac{1}{2}\right) + \frac{C_1' r}{2} + \frac{C_2'}{r} \tag{46}$$

Differentiating gives

$$\frac{d^2\delta}{dr^2} = \frac{3pr^2}{16D} - \frac{pR_i^2}{4D}\left(\ln r + \frac{1}{2}\right) - \frac{R_i r_i}{2D}\left(\ln r + \frac{1}{2}\right)$$

$$+ \frac{C_1'}{2} - \frac{C_2'}{r^2} \qquad (47)$$

Solving for the two constants of integration requires the use of boundary conditions. The slope $d\delta/dr$ at the plate is zero at $r = a$ and $r - b$. Substituting these values into equation (46), the following two equations are obtained. (The two constants can be determined from the two equations.)

$$\frac{-3\ 157\ 280.46}{D} + 39C_1' + 0.01282C_2' = 0$$

and

$$\frac{-1\ 283\ 087.87}{D} + 18C_1' + 0.027777C_2' = 0$$

from which

$$C_1' = \frac{83\ 573.84}{D}$$

and

$$C_2' = -\frac{7\ 964\ 061.58}{D}$$

Therefore

$$\frac{d^2\delta}{dr^2} = \frac{3pr^2}{16D} - \frac{pr_i^2}{4D}\left(\ln r + \frac{1}{2}\right) - \frac{R_i r_i}{2D}\left(\ln r + \frac{1}{2}\right)$$

$$+ \frac{83\ 573.84}{D} + \frac{7\ 964\ 061.58}{Dr^2}$$

Solving for M_r at $r = r_o$ and $r = r_i$ ($d\delta/dr = 0$ at these two points)

$$M_{r,r=r_o} = -1853 \text{ in-lb/in.}$$

and

$$M_{r,r=r_i} + -2727 \text{ in-lb/in.}$$

The negative sign indicates tension on the top surface.

By inspection, it is evident that the moment is positive in the region between $r = r_o$ and $r = r_i$ because the bottom surface is in tension. To obtain the point at which this change is maximum, the derivative of the moment expression, equation (43) is set equal to zero. The value of r that satisfies this equation is determined, and the magnitude of the moment at this point is determined and compared to the moment at $r = r_i$ to obtain the maximum moment in the plate.

$$\frac{d(Mr)}{dr} = -D\left[\frac{d^3\delta}{dr^3} + \nu\left(\frac{1}{r}\frac{d^2\delta}{dr^2} - \frac{1}{r^2}\frac{d\delta}{dr}\right)\right] \tag{48}$$

$$\frac{d^3\delta}{dr^3} = \frac{6pr}{16D} - \frac{pr_i^2}{4D}\left(\frac{1}{r}\right) - \frac{R_i r_i}{2D}\left(\frac{1}{r}\right) - \frac{(2)(7\ 964\ 061.58)}{Dr^3} \tag{49}$$

Substituting equations (46), (47), and (49) into equation (48) with the proper values of p, r_i, and R_i and using $\nu = 0.3$, the following fourth-order equation results.

$$r^4 - 2560.83r^2 - 1\ 838\ 744.376 = 0 \tag{50}$$

Solving equation (50), $r = 56.08$. Substituting this value into equation (43) gives

$$M_{r,r=56.08} = +803 \text{ in-lb/in.}$$

Therefore, the maximum moment is at $r = r_i$ and is

$$M_{max.} = 2727 \text{ in-lb/in.}$$

Examining the magnitude of the reaction loading, R_o - 268 lb/in. (ref. 14). The equation $R_i = 399$ lb/in., determined from equation (45), is the maximum shear loading. Therefore

$$M_{max.} = 2727 \text{ in-lb/in.}$$

and

$$Q_{max.} = 399 \text{ lb/in.}$$

From reference 9, the following stress equations are used.

$$\sigma_f = \frac{E_f z M}{B} \tag{51}$$

and

$$\tau_c = \frac{Q}{t_c + t_f} \tag{52}$$

where σ_f = face sheet stress

τ_c = core shear stress

$$B = \frac{1}{2} E_f t_f \left(t_c + t_f\right)^2$$

$$z = \frac{t_c}{2} + t_f$$

Using core material with $\tau_c = 200$ psi, a density of 4.4 lb/ft^3, and a factor of safety of 1.5

$$\tau_c = 200\left(\frac{1}{1.5}\right) = \frac{Q}{t_c + t_f}$$

$$t_c + t_f = \frac{Q(1.5)}{200} = \frac{1.5(399)}{200}$$

$$t_c + t_f = 3.0 \text{ in.}$$

$$\sigma_f = \frac{E_f z M}{B} = \frac{E_f\left(\frac{t_c + 2t_f}{2}\right)M(2)}{E_f t_f\left(t_c + t_f\right)^2} \tag{53}$$

If face sheets of 2219 aluminum and a safety factor of 1.5 are used, then

$$\sigma_{f,y} = 20\ 000$$

$$20\ 000 = \frac{M\left(t_c + 2t_f\right)}{t_f\left(t_c + t_f\right)^2} \tag{54}$$

Substituting equation (53) into the denominator of equation (54) gives

$$180\ 000\ t_f = M\left(t_c + 2t_f\right)$$

$$\frac{t_c + 2t_f}{t_f} = \frac{180\ 000}{2727} = 132$$

$$t_c = 130t_f$$

From equation (53)

$$t_c = 3.0 - t_f$$

$$131t_f = 3.0$$

$$t_f = 0.046$$

Therefore, use $t_f = 0.05$ inch and $t_c = 2.95$ inches.

The expression for the weight of this sandwich flat plate is

$$W = 2\rho_f \pi \left(r_o^2 - r_i^2\right)\left(t_f\right) + \rho_c \pi \left(r_o^2 - r_i^2\right)\left(t_c\right) \tag{55}$$

$$\rho_f = 0.1 \text{ lb/in}^3$$

$$\rho_c = 4.4 \text{ lb/ft}^3$$

$$W = 2(0.1)(\pi)\left(78^2 - 36^2\right)(0.050) + \frac{4.4(\pi)\left(78^2 - 36^2\right)(2.95)}{(12)^3}$$

$$W = 263 \text{ lb}$$

Rings line the inner and outer surfaces of the plate to serve as interface bands that are welded to the outer wall. Simple rectangular sections are used, and a weight analysis is performed on cross sections for these bands. The general diagram for this plate is shown in figure 22. The cross section of the bands is selected to be 0.125 by 5.0 inches; the material is 2219 aluminum. The weight of the bands is

$$W = (0.125)(5.0)(2\pi)(a + b)\rho$$

$$W = (0.125)(5.0)(2\pi)(114)(0.1)$$

$$W = 45 \text{ lb}$$

The total weight of the sandwich flat-plate closure is computed by adding the weight of the sandwich flat plate to the weight of the bands.

$$W = 263 + 45$$

$$W = 308 \text{ lb}$$

7.4.6 Conical-Shell Bulkhead

7.4.6.1 General.- A conical-shell bulkhead is included for analysis because the pressure loading and tunnel loading are reacted by the same structure. This simple and straightforward analysis is one in which a relatively thin skin of constant thickness in the shape of a conical frustrum is used to connect the tunnel to the outer wall. The need for hatches is recognized, but consideration of hatches is omitted from this evaluation. The tunnel loading, approximately 570 000 pounds, acts as tensile loading on the conical-shell bulkhead. The pressure acts in either direction; however, the pressure acts only to put the shell in compression when the tunnel loading is present and to put the shell in tension when the tunnel loading is not present. Also, because the pressure does not act under normal operation, the only loading present is the tunnel loading. Because of the magnitude of the tunnel loading, it is evident that the more critical loading case exists when the tunnel loading is present.

The analysis includes the examination of the maximum tensile loading (which is caused only by tunnel loading) and sizing the cone accordingly. The magnitude of the compressive stresses is determined, although these stresses do not influence the sizing initially. Circumferential buckling should not be a problem because of the high tensile loading; however, buckling in the meridional direction possibly may occur.

7.4.6.2 Analysis.- Only equilibrium loads are considered during the initial analysis in which conservative results are sought. If the total weight appears to be competitive, a more accurate analysis will be performed to determine if a buckling problem exists and if a weight increase is needed to compensate for discontinuity loads at the cone/cylinder interface.

From figures 23 and 24

$$N_{\phi,x} \cos \phi \left(2\pi r_x\right) = N_{\phi,i}\left(2\pi r_i\right)$$

$$N_{\phi,x} = \frac{N_{\phi,i} r_i}{\cos \phi r_x}$$

$$r_x = x \sin \phi \qquad r_i \sin \phi < x < r_o \sin \phi$$

$$N_{\phi,x} = \frac{N_{\phi,i} r_i}{x \sin \phi \cos \phi}$$

The $N_{\phi,x}$ is maximum for the minimum value of x where $x = r_i \sin \phi$.

$$N_{\phi,max.} = \frac{N_{\phi,i} r_i}{r_i \sin^2 \phi \cos \phi}$$

$$N_{\phi,max.} = \frac{N_{\phi,i}}{\sin^2 \phi \cos \phi} \tag{56}$$

The angle of the cone is a variable that must be considered. The greater the cone angle, the larger the radial loads into the rings that are located in the tunnel and outer wall. Because the analysis is for comparative purposes, it is acceptable to investigate the optimum design even though such investigation would be impractical for other reasons. The conical-section analysis, therefore, considers the optimum design. The angle that gives the minimum weight is selected and the weight is used for comparison. If the cone is competitive, then refinements will be made to the analysis to provide realistic results; otherwise, the conical-shell design will be eliminated.

$$W = A_s t \rho \tag{57}$$

$$A_s = \pi l \left(r_i + r_o \right) \tag{58}$$

If l equals the length of the side and

$$l = \frac{r_o - r_i}{\sin \phi}$$

then

$$A_s = \frac{\pi\left(r_i + r_o\right)\left(r_o - r_i\right)}{\sin \phi} \tag{59}$$

From equation (56)

$$\sigma_{\phi,max.} = \frac{N_{\phi,max.}}{t} = \frac{N_{\phi,i}}{t \sin^2\phi \cos \phi}$$

$$\sigma_{\phi,max.} = \frac{\sigma_y}{fs} = \frac{30\ 000}{1.5} = 20\ 000 \text{ psi}$$

$$t = \frac{N_{\phi,i}}{\sigma_{\phi,max.} \sin^2\phi \cos \phi} \tag{60}$$

Substituting equations (59) and (60) into equation (57)

$$W = \frac{\pi\left(r_o + r_i\right)\left(r_o - r_i\right)}{\sin \phi}\left(\frac{N_{\phi,i}}{\sigma_{\phi,max.} \sin^2\phi \cos \phi}\right)\rho$$

$$W = \frac{N_{\phi,i}\rho\pi\left(r_o + r_i\right)\left(r_o - r_i\right)}{\sigma_{\phi,max.}}\left(\frac{1}{\sin^3\phi \cos \phi}\right) \tag{61}$$

The weight is minimum if $\sin^3\phi \cos \phi$ is maximum. To find the maximum value of $\sin^3\phi \cos \phi$

$$\frac{d\left(\sin^3\phi \cos \phi\right)}{d\phi} = 0 = 3 \sin^2 d \cos^2\phi - \sin^4\phi$$

$$3 \sin^2\phi \cos^2\phi = \sin^4\phi$$

$$3 \cos^2\phi = \sin^2 d$$

$$\tan^2\phi = 3$$

$$\tan \phi = \sqrt{3}$$

$$\phi = 60^\circ$$

From equation (61) and using $r_o = 78$, $r_i = 36$, and $\phi = 60^\circ$

$$W_{min.} = \frac{(30\ 191)\left(\frac{1}{12}\right)(0.1)(\pi)(78 + 36)(78 - 36)}{(20\ 000)(0.866)^3(0.5)}$$

$$W_{min.} = 583$$

The absolute minimum weight of the conical-shell closure is approximately equal to the weight of the sandwich flat-plate closure with tension rods. Because of the impractical angle of the cone, the weight presented is unrealistic. A more practical, but not necessarily the best, angle to consider is 45°. The corresponding weight for this conical section would be approximately 750 pounds, which does not include the consideration of any buckling reinforcement or discontinuity loading. If a legitimate analysis of a conical-shell closure were to be accomplished, the shell would not be competitive with the sandwich flat-plate closure with tension rod or possibly with the sandwich flat-plate closure with shear webs. For this reason, the conical-shell closure was eliminated from consideration. However, the magnitude of the compressive hoop loads that exist in the conical shell when LQM 1 is pressurized and when the hub has lost pressure was determined. Although the magnitude of compressive hoop loads is not important to the preliminary analysis, the determination serves to assess compressive-hoop-load influence on the shell.

From reference 10, the relationship between meridional stress and hoop stress in a shell is given by

$$\frac{N_\phi}{r_\phi} + \frac{N_\theta}{r_\theta} = -p \tag{62}$$

Where r_ϕ is the radius of curvature in the meridional direction, r_θ is the radius of curvature in the circumferential direction, N_ϕ and N_θ are the meridional loading and hoop loading, respectively, and p is the pressure loading.

For the conical-shell closure, $r_\phi = \infty$ and $r_\theta = x \tan \phi$

$$N_\theta = -(x)(p)\tan \phi \tag{63}$$

$N_{\theta,max.}$ occurs at maximum x, which is $x = r_\theta/\sin \phi$. Therefore

$$N_{\theta,max.} = \frac{r_\theta p}{\cos \phi}$$

Using $\phi = 45°$

$$N_{\theta,max.} = -1635 \text{ lb/in.}$$

$$N_{\theta,max.} = -19\,620 \text{ lb/ft}$$

This magnitude is more than negligible and would need to be considered if an extended analysis were performed.

7.4.7 Partial Toroidal Closure with Large Radius of Curvature

7.4.7.1 General.- The analysis of the partial toroidal closure must consider the fact that pressure acts from either direction. A full (closed) toroid would not be applicable because of the partial geometry; consequently, only the partial (open) shell is examined. Using reference 13, 0.70 inch is found to be the necessary thickness for an externally pressurized toroidal shell. More information on the semitoroid is available in section 7.4.4.2.

7.4.7.2 Analysis.- Using figure 25, the surface area of the partial toroidal shell is determined as follows:

$$A_s = 2\pi \int_{36}^{0} x \sqrt{1 + \frac{dy^2}{dx}}\, dx$$

$$(x - 111)^2 + y^2 = (75)^2$$

$$y^2 = (75)^2 - (x - 111)^2 = 75^2 - x^2 + 222x - (111)^2$$

$$y^2 = -x^2 + 222x - 6696$$

$$y = \left(-x^2 + 222x - 6696\right)^{1/2}$$

$$\frac{dy}{dx} = \frac{1}{2}\left(-x^2 + 222x - 6696\right)^{-1/2}(-2x + 222)$$

$$\frac{dy}{dx} = \frac{-x + 111}{-x^2 + 222x - 6696^{1/2}}$$

$$\left(\frac{dy}{dx}\right)^2 = \frac{(-x + 111)^2}{-x^2 + 222x - 6696}$$

$$A_s = 2\pi \int_{36}^{78} x \left(1 + \frac{x^2 - 222x + 12321}{-x^2 + 222x - 6696}\right)^{1/2} dx$$

$$A_s = 2\pi \int_{36}^{78} x \left(\frac{-x^2 + 222x - 6696 + x^2 - 222x + 12\,321}{-x^2 + 222x - 6696}\right)^{1/2} dx$$

$$A_s = 2\pi \int_{36}^{78} x \left(\frac{5625}{-x^2 + 222x - 6696}\right)^{1/2} dx$$

$$A_s = 2\pi(5625)^{1/2} \int_{36}^{78} \frac{x\,dx}{\sqrt{-x^2 + 222x - 6696}} \qquad (64)$$

Using integral equation (203) from reference 15

$$A_s = 2\pi(5625)^{1/2} \left[-\left(-x^2 + 222x - 6696\right)^{1/2} + 111 \int \frac{dx}{\sqrt{-x^2 + 222x' - 6696}} \right]_{36}^{78}$$

$$A_s = 2\pi(5625)^{1/2} \left[-\left(-x^2 + 222x - 6696\right)^{1/2} + (111)\sin^{-1}\left(\frac{2x - 222}{150}\right) \right]_{36}^{78}$$

$$A_s = 2\pi(5625)^{1/2} \left[-\left(-x^2 + 222x - 6696\right)^{1/2} + (111)\sin^{-1}\left(\frac{x - 111}{75}\right) \right]_{36}^{78}$$

$$A_s = 2\pi(5625)^{1/2} \left\{ \left[-67.35 + (111)\sin^{-1}(-0.44)\right] - 111\left[0 + (111)\sin^{-1}(-1.0)\right] \right\}$$

$$A_s = 2\pi(5625)^{1/2} \left[-67.35 + 111(-0.46 + 1.57)\right]$$

$$A_s = 26\ 323.5\ in^2$$

The weight (in pounds) is found by multiplying the surface area by the thickness and material density as follows.

$$W = A_s t \rho \tag{65}$$

$$W = (26\ 323.5)(0.7)(0.1)$$

$$W = 1843$$

7.4.8 Summary, Inboard Bulkhead Closure

If weight is the only factor considered, the inboard bulkhead closure that combines tension rods to take tunnel loading and a honeycomb sandwich plate to act as a pressure bulkhead is the optimum configuration. The total weight determined by preliminary analysis is approximately 625 pounds, which is a relatively good estimate of the weight that could be determined by a detailed analysis. The fabrication of this type of closure requires nothing unusual or new; thus, the approach is entirely practical.

Only the presence of tension rods in the cylindrical volume might be objectionable. The position of the tension rods is not expected to be a serious problem. However, if the configuration proved to be unusable for this reason, either the conical shell or partial toroidal shell could be used with a sacrifice in volume and weight. All concepts have been presented to permit further evaluation.

8.0 WEIGHT SUMMARY

The component weights and total weights for the living quarters modules that were computed from the structural analysis and weight-estimating technique are presented in table XVI. The combined weights of LQM 1 and LQM 2, computed after the structural analysis was performed, is 69 438 pounds.

A predicted weight of 99 282 pounds for the two living quarters modules was obtained by the use of a weight-estimating technique during an in-house study of space-base guidelines, ground rules, and configurations in May 1969. Included in this predicted weight are the weights of the hatches, windows, docking rings, and so forth, which were omitted from the current study.

9.0 CONCLUSIONS

The analysis that was performed on the primary structure of the living quarters modules for the earth-orbiting space base has been presented. The pressure-skin thickness, the stringer spacing, and the stringer sections were determined so that failure of each would occur simultaneously. The floors were designed with a double-structure makeup. A network of support beams was designed to carry the entire load to which the floor is subjected. The beams were spanned by aluminum honeycomb panels that distribute a uniform type of load to the beams. Concentrated loadings were carried directly into the beams. The tunnel thickness was determined so as to withstand both internal and external pressure. In addition to withstanding pressure differential, the tunnel acted as a tension-tie between the end-bulkhead closures.

The end-bulkhead closures consisted of three semitoroidal shells with elliptical cross sections (for which the tunnel and outer wall are boundaries) and one flat-plate aluminum honeycomb closure. The toroidal closures were relatively thinskinned shells designed for the existence of membrane-type loadings. The flat-plate closure, reacting only pressure at the small diameter end of living quarters module 1, was supplemented by tension rods to counteract tunnel loading. The tunnel at the outboard end of living quarters module 2 was closed off by a slightly ellipsoidal shell.

In summary, the preliminary design determined by this study reflects a minimum-weight structure that is based not only on theoretical stress analysis but also, to a large extent, on empirical data and formulations. The design material and manufacturing requirements are entirely feasible, and a good base-line design from which the final space-base structure could evolve has been provided. The weight computed after the structural analysis was performed is approximately 30 percent less than the predicted weight. However, this value is within the range of weight desired if weight is added for hatches, windows, docking rings, and so forth, which were omitted from the analysis. Therefore, it is concluded that the accuracy of the weight-estimation technique is acceptable.

10.0 REFERENCES

1. Vale, Robert: Manned Spacecraft: Engineering Design and Operations. Spacecraft Structural Concepts, ch. 9, P. E. Purser, M. A. Faget, and N. F. Smith, eds., Fairchild Publications, Inc. (New York), 1964.

2. Card, M. F.; and Jones, R. M.: Buckling of Axially Compressed Cylinders with Eccentric Longitudinal Stiffeners. Technical Papers, 7th Structures and Materials Conference, Inst. of Aeron. and Astronaut. and Am. Society of Mech. Engrs., Cocoa Beach, Fla., Apr. 18-20, 1966. Am. Inst. Aeron. and Astronaut. (New York), 1966, pp. 23-24.

3. Block, D. L.; Card, M. F.; and Mikulas, M. M., Jr.: Buckling of Eccentrically Stiffened Orthotropic Cylinders. NASA TN D-2960, 1965.

4. Hofer, K. E., Jr.: Equations for Fracture Mechanics. Machine Design, vol. 40, no. 3, Feb. 1968, pp. 109-113.

5. Baker, E. H.; Cappelli, A. P.; Kovalevsky, L.; Rish, F. L.; and Verette, R. M.: Shell Analysis Manual. NASA CR-912, 1968.

6. Paterson, J. P.; and Dow, M. B.: Compression Tests on Circular Cylinders Stiffened Longitudinally by Closely Spaced Z-Section Stringers. NASA Memo 2-12-59L, 1959.

7. Anon.: Alcoa Structural Handbook, A Design Manual for Aluminum. Aluminum Co. of America (Pittsburgh, Pa.), 1960.

8. Roark, Raymond J.: Formulas for Stress and Strain. Fourth ed., McGraw-Hill Book Co., 1965.

9. Plantema, Frederik J.: Sandwich Construction. John Wiley & Sons, Inc., 1966.

10. Timoshenko, S.; and Woinowsky-Krieger, S.: Theory of Plates and Shells. Second ed., McGraw-Hill Book Co., Inc., 1959.

11. Turner, Harry M.: Design Parameters for Elliptical Toroidal Pressure Vessels. Aerospace Eng., vol. 21, no. 11, Nov. 1962, pp. 33-38.

12. Baumeister, Theodore, ed.: Marks' Mechanical Engineers' Handbook. Sixth ed., McGraw-Hill Book Co., Inc., 1958.

13. Sobel, L. H.; and Flügge, W.: Stability of Toroidal Shells under Uniform External Pressure. AIAA J., vol. 5, no. 3, Mar. 1967, pp. 425-431.

14. Griffel, William: Plate Formulas. Frederick Ungar Pub. Co. (New York), 1968.

15. Anon.: C. R. C. Standard Mathematical Tables. Twelfth ed., Chemical Rubber Pub. Co. (Cleveland, Ohio), 1959.

TABLE I.- LIVING QUARTERS MODULE I EXTERNAL LOADS

Floor	Case I (a)		Case II (b)		Case III (c)	
	Axial load, lb	Moment, in-lb	Axial load, lb	Moment, in-lb	Axial load, lb	Moment, in-lb
3	23×10^4	33×10^6	9.2×10^5	27.5×10^7	11.5×10^5	6.2×10^6
2	17	26	8.25	19.5	8.5	4.25
1	11	20	7.5	15.7	5.05	2.75
0	8	16	6.2	12	4	2
-1	7	12	4.5	9	3	1.2
-2	4	8	3	6.75	2	1
-3	3	6	2	4.5	1.6	.75
[d]-4	2.8	4	1	3.75	1.2	.25
[d]-5	2.7	2	.7	2.25	1	.1
[d]-6	1.8	1	.7	1.5	.5	≈0

[a]Free-standing ground winds.

[b]Maximum $q\alpha$.

[c]First-stage end boost.

[d]Rings only.

TABLE II.- EXTERNAL LOADS CAUSED

BY INTERNAL PRESSURE

LQM 1 floor	Average radius, in.	N_o/p, in.
3	178	52.2
2	167	48.3
1	151	42.9
0	142	39.8
-1	132	36.4
-2	122	32.8
-3	91	21.9
-4	91	21.9
-5	91	21.9
-6	91	21.9

TABLE III.- LIMIT LOADS FOR LQM 1

Floor	Limit compression load, lb/in.	Limit tension load, lb/in.
3	3038	2540
2	2481	1990
1	2518	1880
0	2152	1637
-1	1786	1503
-2	1474	1414
-3	1798	1662
[a]-4	1335	1548
[a]-5	695	1014
[a]-6	410	729

[a]Ring only.

TABLE IV.- DESIGN LOADS FOR LQM 1

Floor	Compression load, lb/in.	Tension load, lb/in.
3	6076	3810
2	4962	2985
1	5036	2820
0	4304	2455
-1	3572	2255
-2	2948	2121
-3	3596	2493
[a]-4	2670	2322
[a]-5	1390	1521
[a]-6	820	1094

[a]Ring only.

TABLE V.- STRINGER SPACING AND NUMBER OF STRINGERS PER FLOOR FOR LQM 1

Floor	Stringer spacing, u, in.	No. of stringers
3	8.15	137
2	9.20	114
1	9.2	103
0	9.9	76
-1	11.7	71
-2	17.03	45
-3	11.9	48
[a]-4	15.5	37
[a]-5	16.8	34
[a]-6	(b)	(b)

[a]Ring only.

[b]No stringer required.

TABLE VI.- STRINGER CROSS-SECTION PROPERTIES FOR LQM 1

Floor	A_{str}, in^2	I_{str}, in^4	W_{str}, lb	Total stringer weight, lb
3	1.86	4.37	20.1	2753
2	1.67	3.69	18.0	2052
1	1.65	3.62	17.8	1833
0	1.21	3.08	13.1	996
-1	1.07	2.57	11.6	823
-2	.97	2.42	10.5	472
-3	.78	1.73	8.4	403
[a]-4	.67	.89	7.2	266
[a]-5	(b)	(b)	(b)	(b)
[a]-6	(b)	(b)	(b)	(b)
Total				9599

[a]Ring only.

[b]No stringer needed.

TABLE VII.- EXTERNAL LOADS FOR LQM 2

Floor	Case I (a)		Case II (b)		Case III (c)	
	Axial load, lb	Moment, in-lb	Axial load, lb	Moment, in-lb	Axial load, lb	Moment, in-lb
5	2.2×10^5	4.1×10^7	5.5×10^5	1.75×10^8	1×10^6	6×10^6
4	1.9	3.5	4.8	1.4	.85	4
3	1.3	2.7	4.5	1.2	.75	3
2	1.1	2	3.9	9.9	.6	2
1	.75	1.1	3	8	.4	.9

[a]Free-standing ground winds.

[b]Maximum $q\alpha$.

[c]First-stage end boost.

TABLE VIII.- LIMIT LOADS FOR LQM 2

Floor	Limit compression load, lb/in.	Limit tension load, lb/in.
5	1618	1881.9
4	1208	1592
3	982	1417.5
2	721	1259
1	454	1145.8

TABLE IX.- DESIGN LOADS FOR LQM 2

Floor	Design compression load, lb/in.	Design tension load, lb/in.
5	3236	2822
4	2416	2387
3	1964	2126
2	1442	1888
1	908	1718.7

TABLE X.- STRINGER SPACING AND NUMBER OF STRINGERS PER FLOOR FOR LQM 2

Floor	Stringer spacing, u, in.	No. of stringers
5	10.9	107
4	13.3	88
3	15.6	75
2	22	53
1	(a)	(a)

[a]No stringer required.

TABLE XI.- STRINGER CROSS SECTIONS FOR LQM 2

Floor	A_{str}, in^2	I_{str}, in^4	W_{str}, lb	Total stringer weight, lb
5	1.007	2.56	10.87	1163
4	.84	1.94	9.07	798
3	.72	1.48	7.77	583
2	.56	.90	6.04	320
1	(a)	(a)	(a)	(a)
Total				2864

[a]No stringer required.

TABLE XII.- FLOOR BEAM DATA

Beam	Quantity	l, in.	w, lb/in.	M, in-lb	V, lb	S, in^3	I-beam data	A, in^2	I, in^4	W, lb
36-inch spacing										
1	2	150	62	116 250	4650	1.162	3 × 2.33	1.67	2.52	80
2	4	180	62	167 400	5580	1.674	3 × 2.33	1.67	2.52	192
3	2	340	62	597 267	10 540	5.97	5 × 3.284	4.34	15.22	472
4	2	300	62	465 000	9300	4.65	5 × 3.00	2.92	12.26	280
5	2	230	62	273 317	7130	2.733	4 × 2.66	2.25	6.06	166
6	2	80	62	33 067	2480	.331	3 × 2.33	1.67	2.52	43
Total										1233
40-inch spacing										
1	4	153	69	134 602	5279	1.346	3 × 2.33	1.67	2.52	164
2	2	350	69	704 375	12 075	7.044	6 × 3.33	3.66	22.08	410
3	2	310	69	552 575	10 695	5.526	5 × 3.137	3.60	13.69	357
4	2	243	69	339 532	8384	3.40	4 × 2.796	2.79	6.79	217
5	2	90	69	46 575	3105	.466	3 × 2.33	1.67	2.52	48
Total										1196

TABLE XII.- FLOOR BEAM DATA - Continued

Beam	Quantity	l, in.	w, lb/in.	M, in-lb	V, lb	S, in^3	I-beam data	A, in^2	I, in^4	W, lb
44-inch spacing										
1	4	155	76	152 158	5 890	1.52	3 × 2.33	1.67	2.52	166
2	2	346	76	758 201	13 148	7.58	6 × 3.443	4.34	24.11	481
3	2	300	76	570 000	11 400	5.7	5 × 3.284	4.34	15.22	417
4	2	210	76	279 300	7 980	2.79	4 × 2.66	2.25	6.06	151
Total										1215
48-inch spacing										
1	4	155	83	166 173	6 433	1.66	3 × 2.33	1.67	2.52	166
2	2	340	83	799 567	14 110	7.996	6 × 3.443	4.34	24.11	472
3	2	280	83	542 267	11 620	5.423	5 × 3.137	3.60	13.69	322
4	2	160	83	177 067	6 640	1.771	3 × 2.411	1.91	2.71	98
Total										1058

TABLE XII.- FLOOR BEAM DATA - Concluded

Beam	Quantity	l, in.	w, lb/in.	M, in-lb	V, lb	S, in^3	I-beam data	A, in^2	I, in^4	W, lb
52-inch spacing										
1	4	155	90	180 188	6 975	1.802	3 × 2.411	1.91	2.71	189.5
2	2	336	90	846 720	15 120	8.467	6 × 3.565	5.07	26.31	545.1
3	2	265	90	526 688	11 925	5.267	5 × 3.137	3.60	13.69	305.3
Total										1039.9
72-inch spacing										
1	4	150	124	232 500	9 300	2.325	4 × 2.66	2.25	6.06	216
2	2	300	124	930 000	18 600	9.30	7 × 3.66	4.48	36.69	430
Total										646

TABLE XIII.- HONEYCOMB-PANEL DATA

u, in.	M, in-lb/in.	t_f, in.	t_c, in.	τ_c, psi	D, in-lb	S, in^3	δ, in.	Unit weight, lb/ft^2	W, lb
36	186	0.020	0.45	65.87	25 488	12.567	0.32	0.745	540
40	229	.020	.55	60.4	37 488	15 123	.33	.782	567
44	277	.020	.67	54.84	54 935	18 191	.33	.827	600
48	330	.020	.81	49.73	79 488	21 773	.32	.880	638
52	387	.020	.95	46.1	108 565	25 355	.32	.932	676
56	449	.020	1.10	43	144 738	29 193	.33	.989	717
60	516	.020	1.27	40	192 012	33 544	.33	1.052	763
64	587	.020	1.45	37.4	249 335	38 151	.32	1.120	812
68	662	.020	1.64	35.2	317 954	43 014	.32	1.191	863
72	742	.020	1.84	33.2	399 185	48 134	.32	1.266	918

TABLE XIV.- FLOOR-WEIGHT SUMMARY

u, in.	Beam weight, lb	Honeycomb weight, lb	Total weight, lb
36	1233	540	1773
40	1196	567	1763
44	1215	600	1815
48	1058	638	1696
52	1040	676	1716
72	646	918	1564

TABLE XV.- TENSION-ROD DATA

θ, deg	Total rod weight, W, lb	Radial load, F_h, lb	Extended distance, e, in.
45	76.5	56 909	42
35	81.4	39 848	60
25	99.8	26 537	90
20	119	20 713	115
15	153	15 249	157
10	224	10 035	238
7	316	6 988	342
5	440	4 979	480

TABLE XVI.- WEIGHT SUMMARY

Component	LQM 1 weight, lb	LQM 2 weight, lb
Outside wall	22 056	14 344
Floor	5 088	8 480
Tunnel	8 334	3 906
Tunnel closure	--	66
Toroidal bulkhead	2 180	4 360
Flat bulkhead	624	--
Total	38 282	31 156

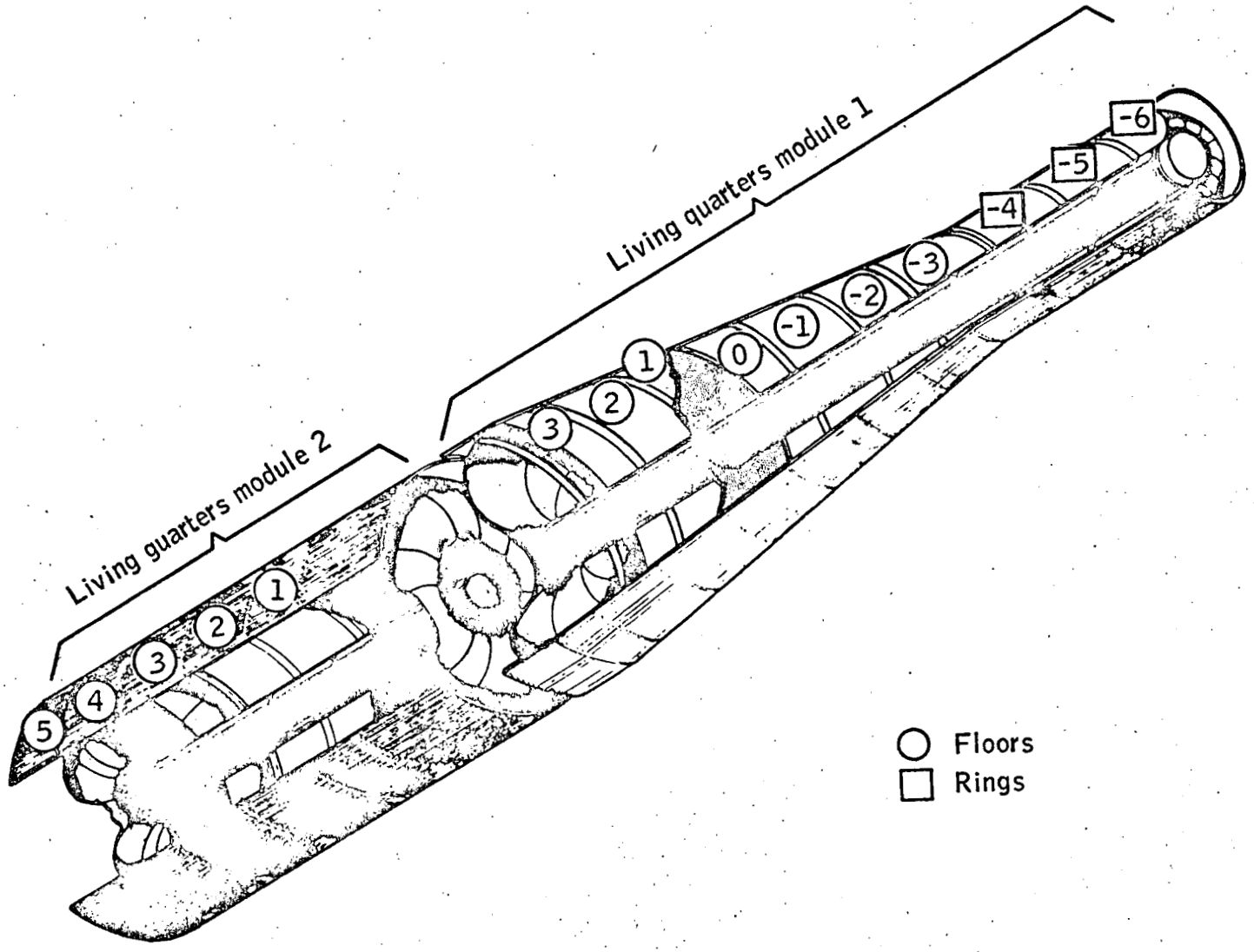

Figure 1.- Structural configuration of the earth-orbiting space base.

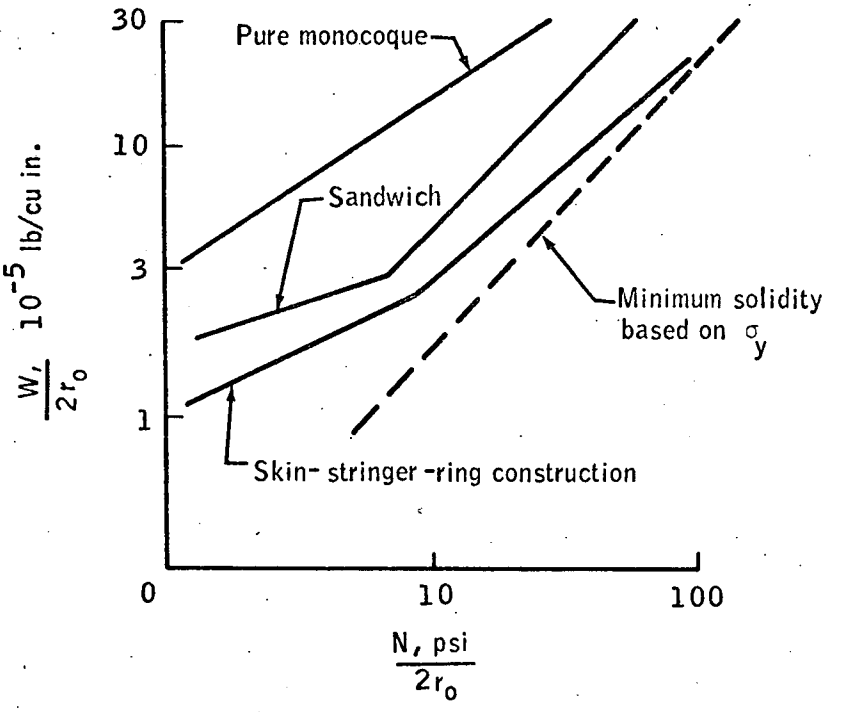

Figure 2.- Structural efficiency for lightly pressurized cylindrical shells under longitudinal compression.

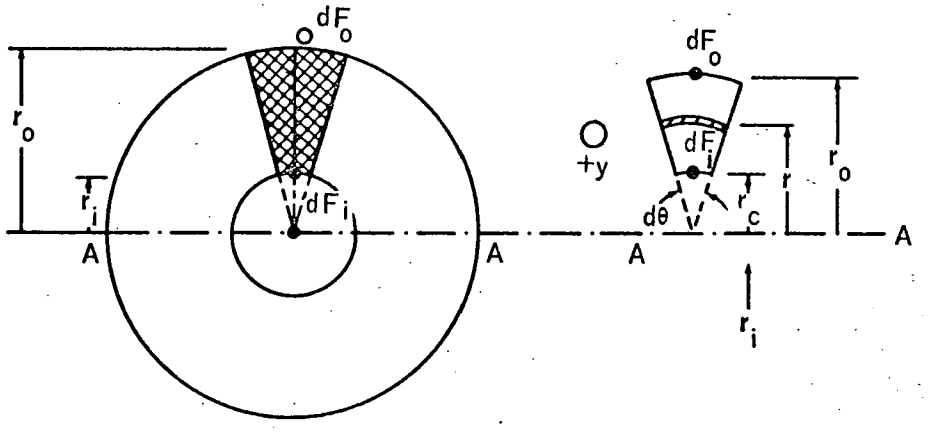

Figure 3.- Free-body diagram of pressure loads.

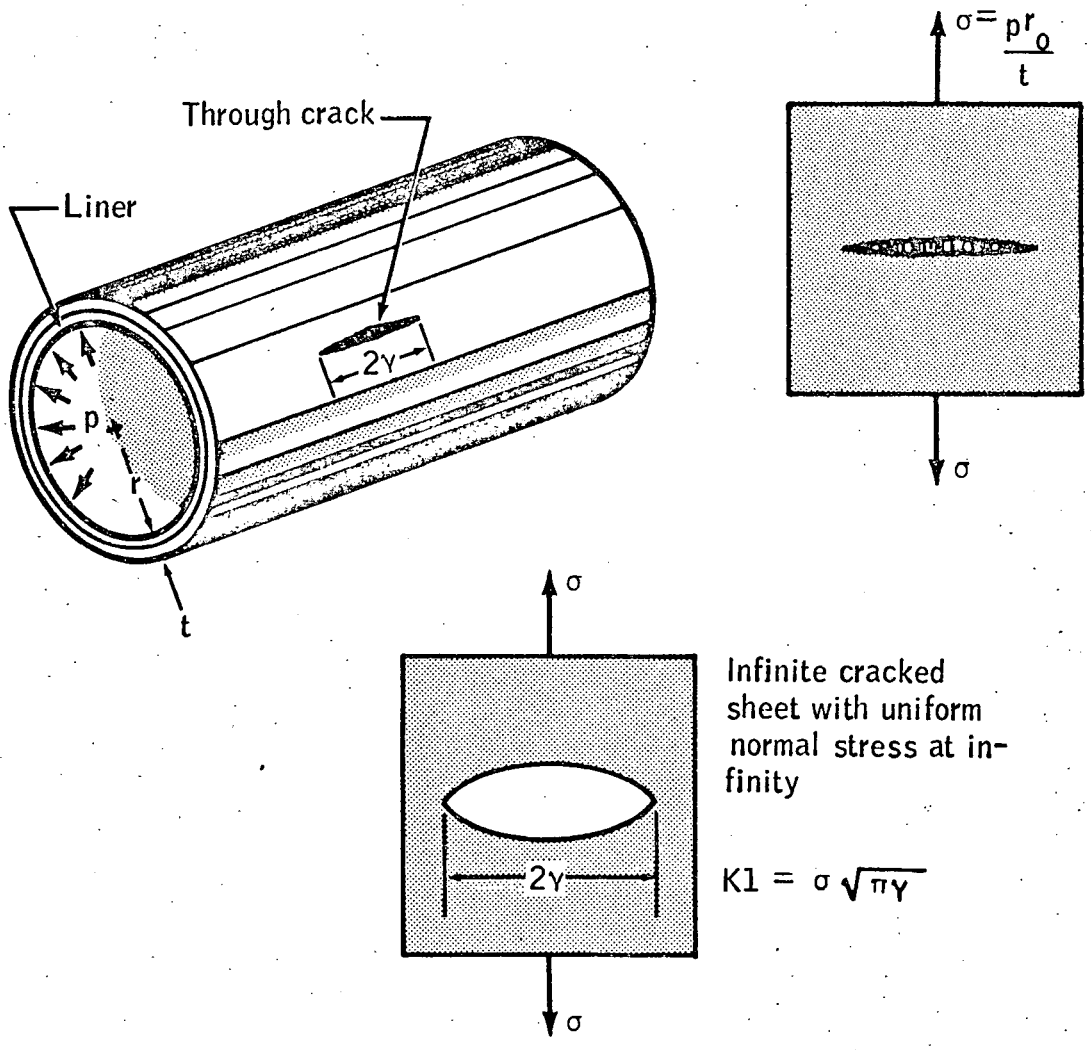

Figure 4.- Cylinder under pressure.

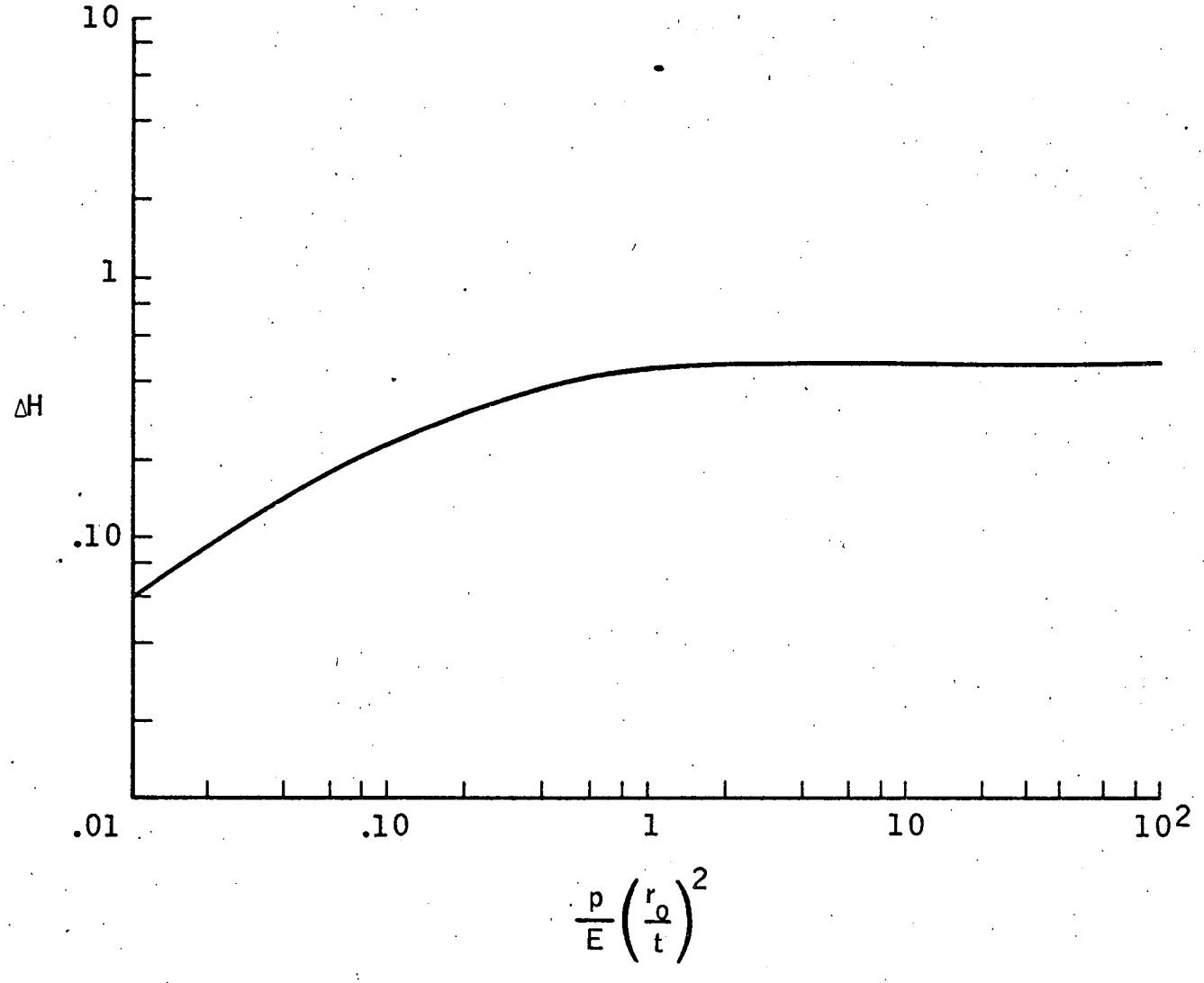

Figure 5.- Increase in axial-compressive buckling-stress coefficient of curved panels caused by internal pressure.

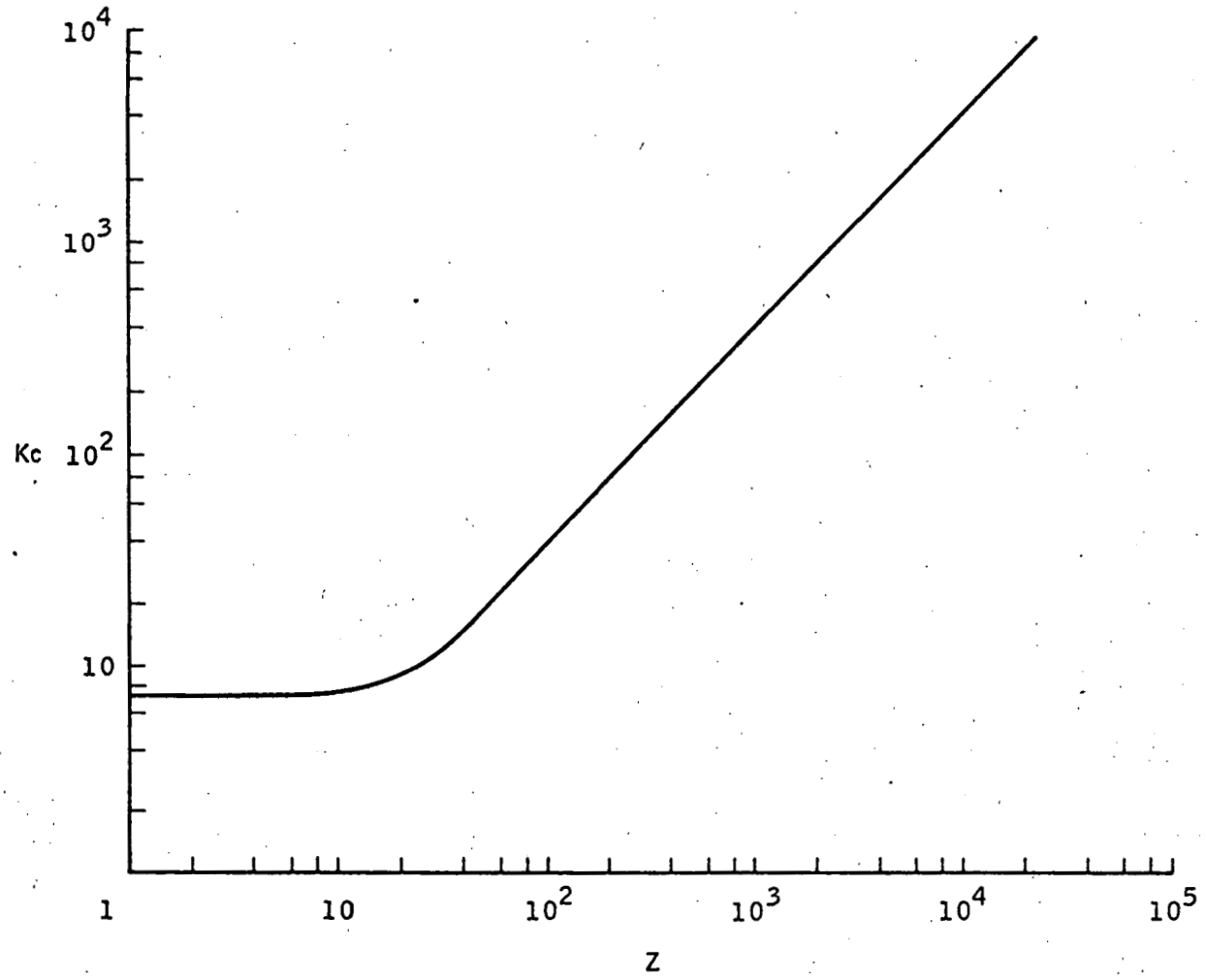

Figure 6.- Buckling-stress coefficient Kc for unpressurized curved panels subjected to axial compression.

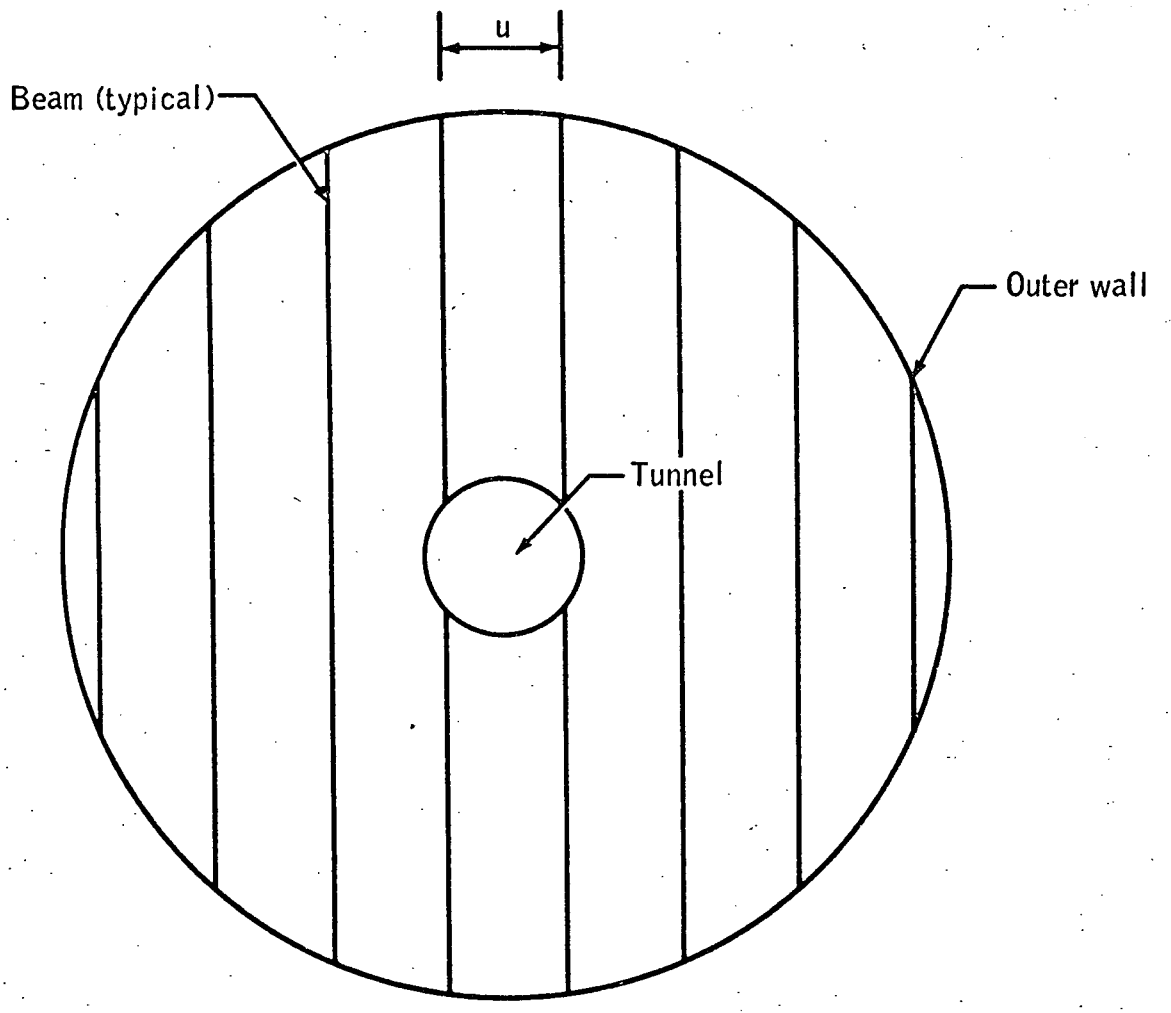

Figure 7.- Floor-beam arrangement.

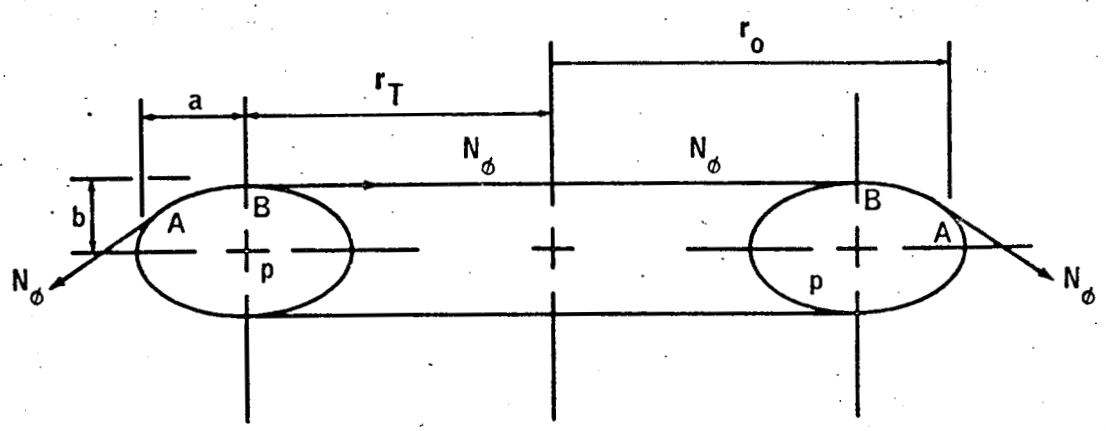

Figure 8.- Elliptical-torus geometry.

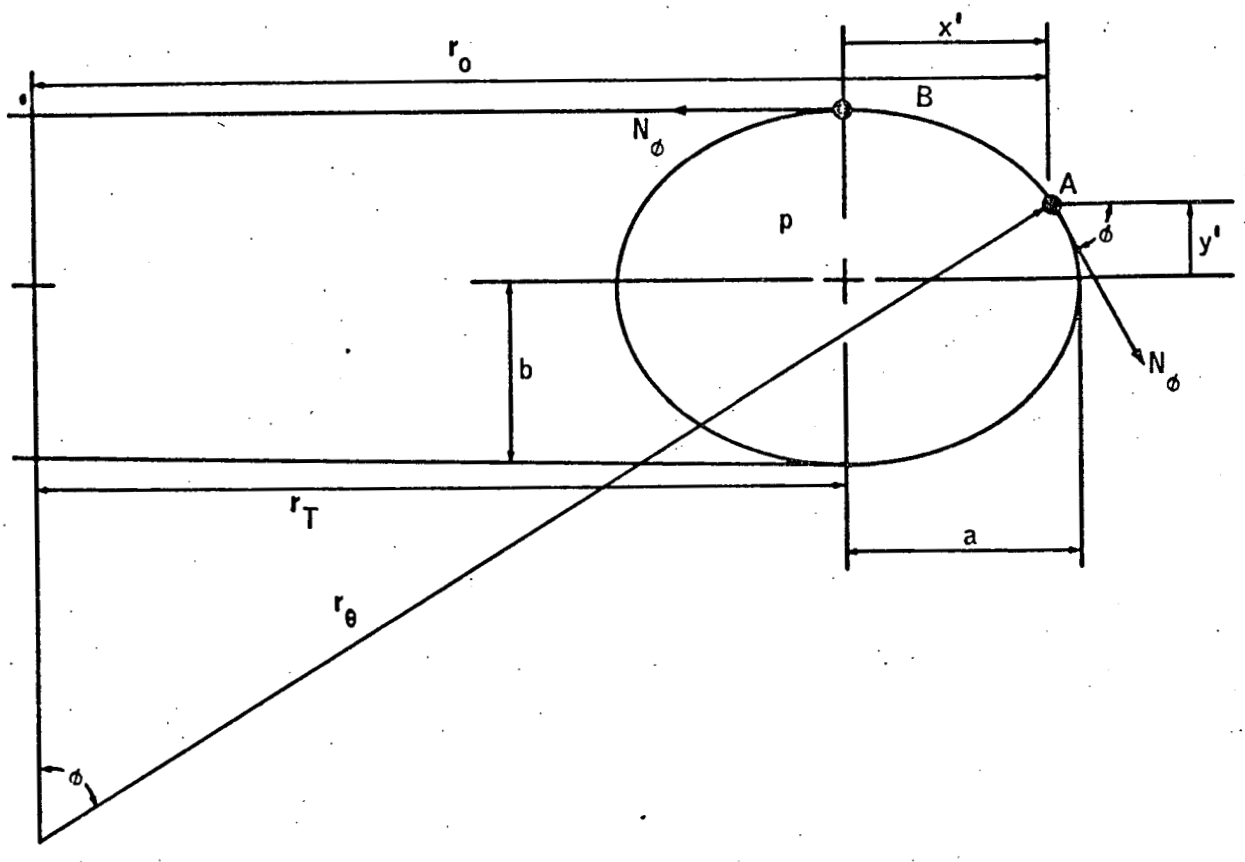

Figure 9.- Elliptical torus, radii of curvature.

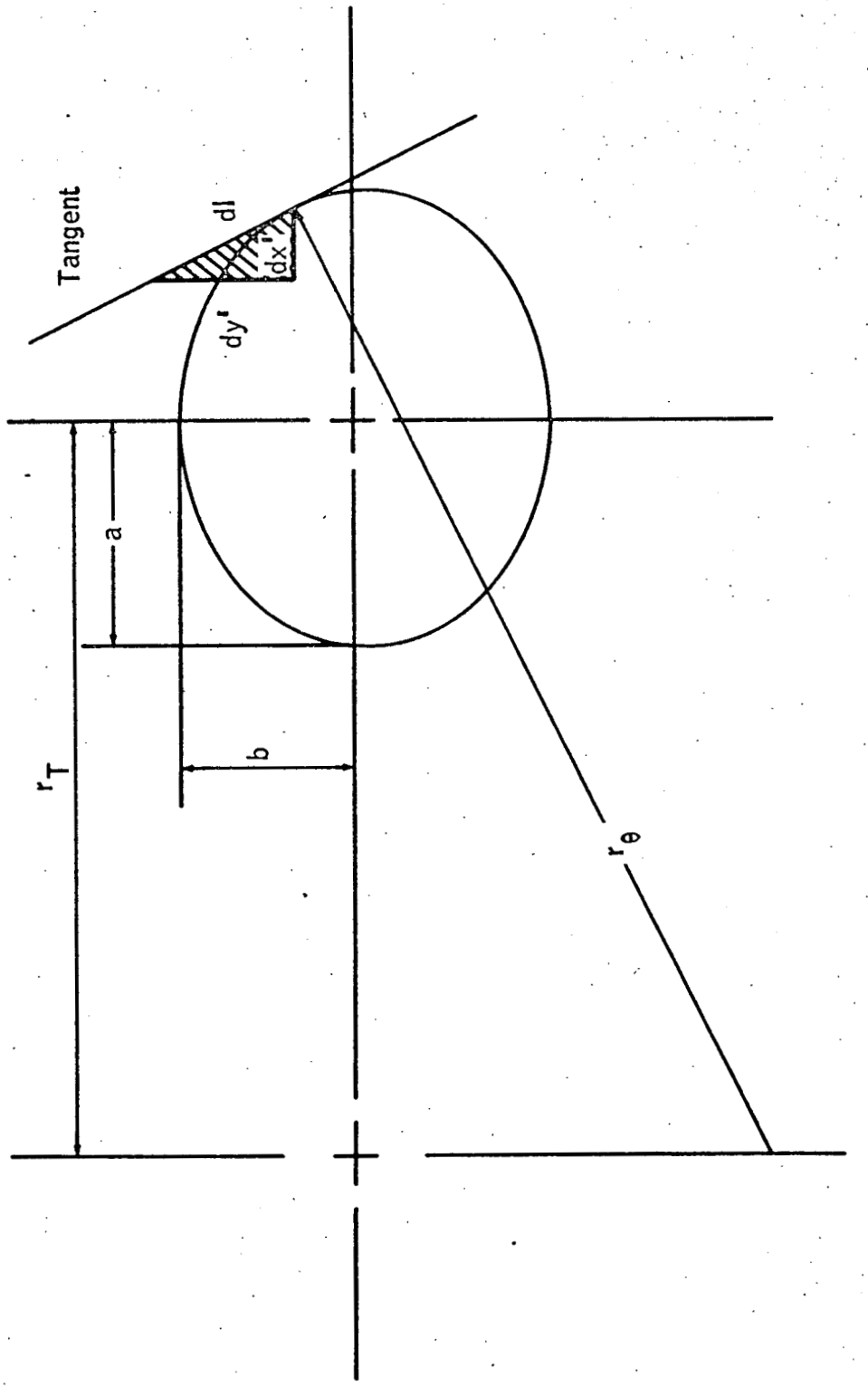

Figure 10.- Elliptical torus.

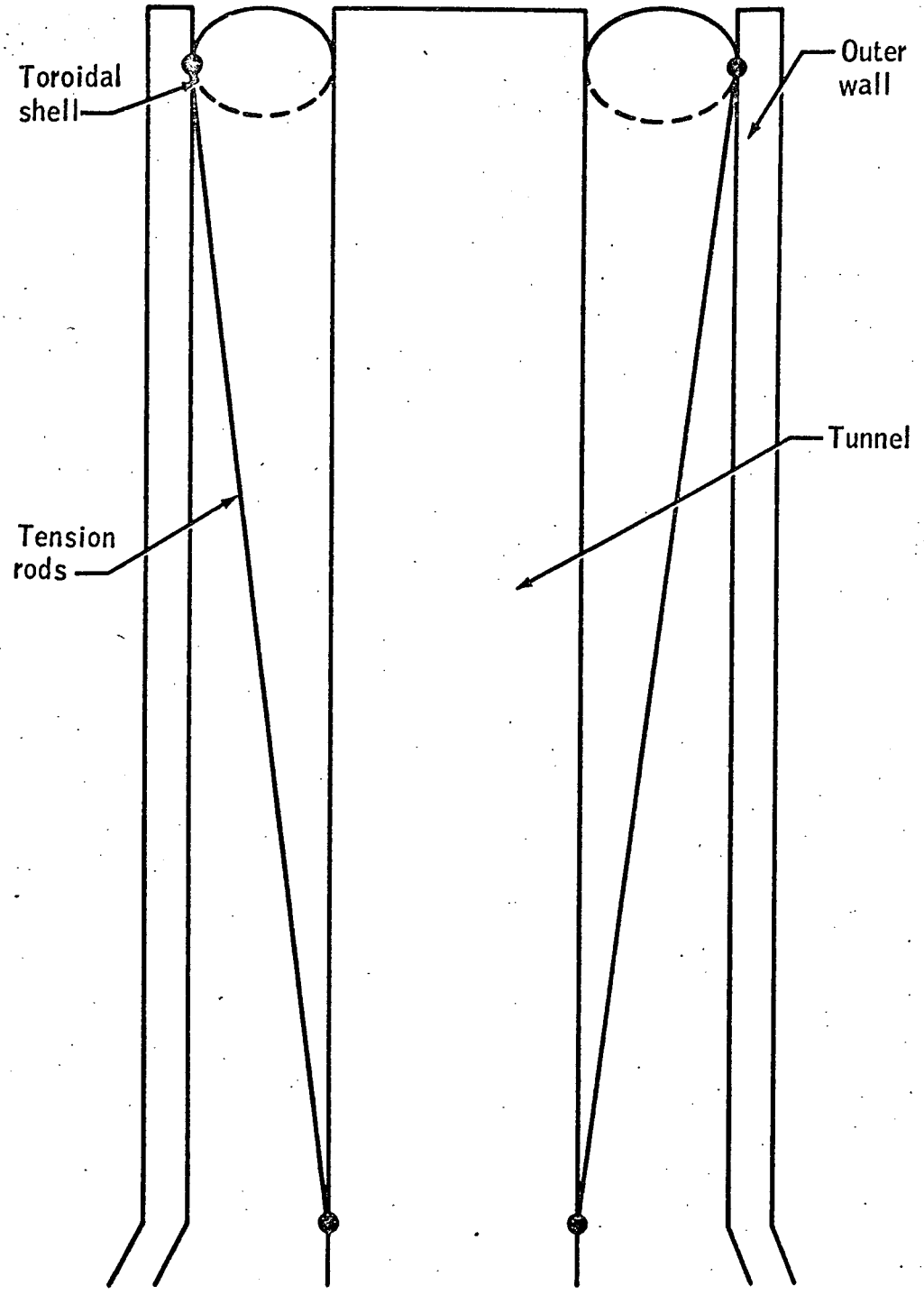

Figure 11.- Toroidal shell with tension rods.

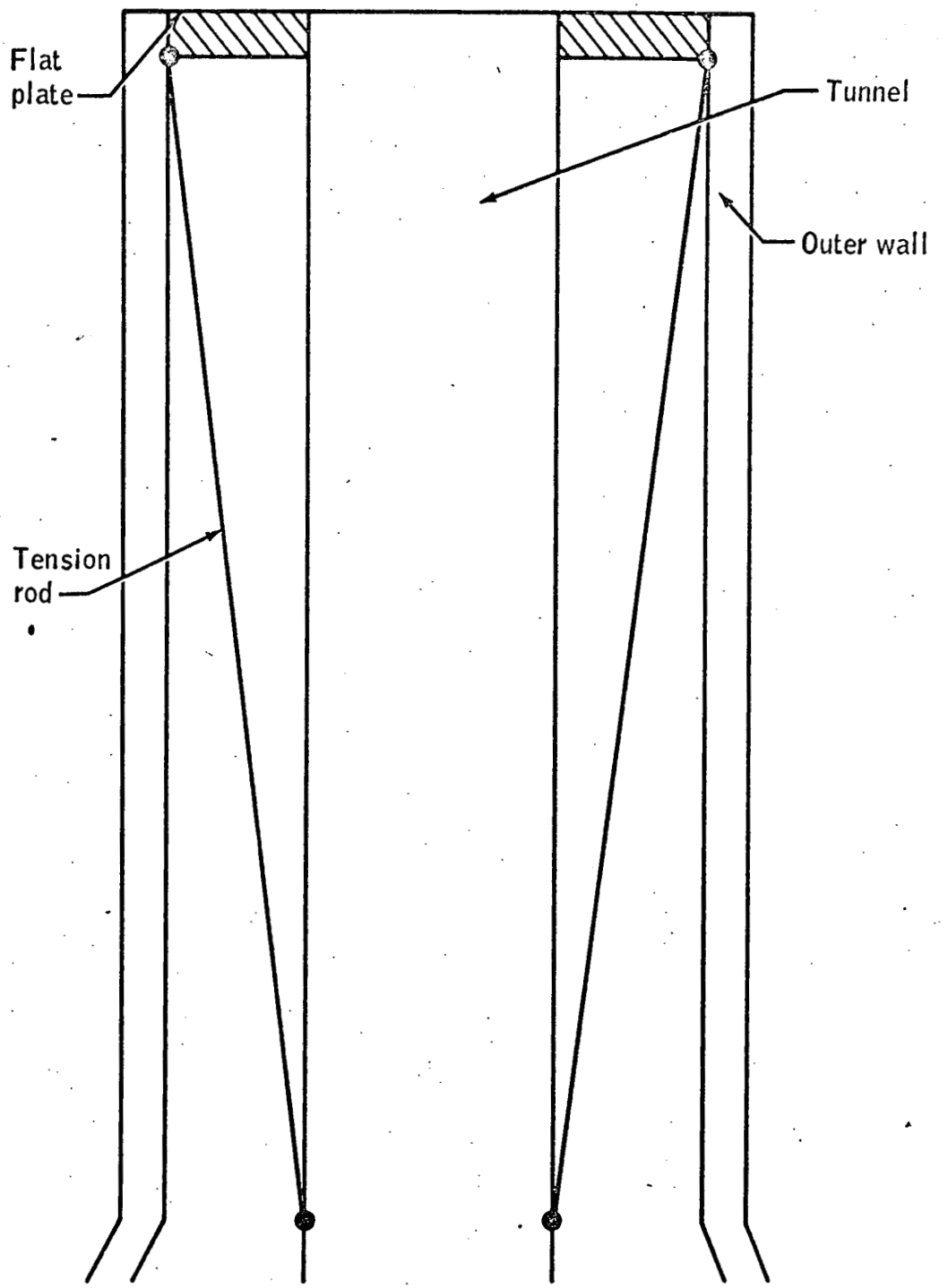

Figure 12.- Flat plate with tension rods.

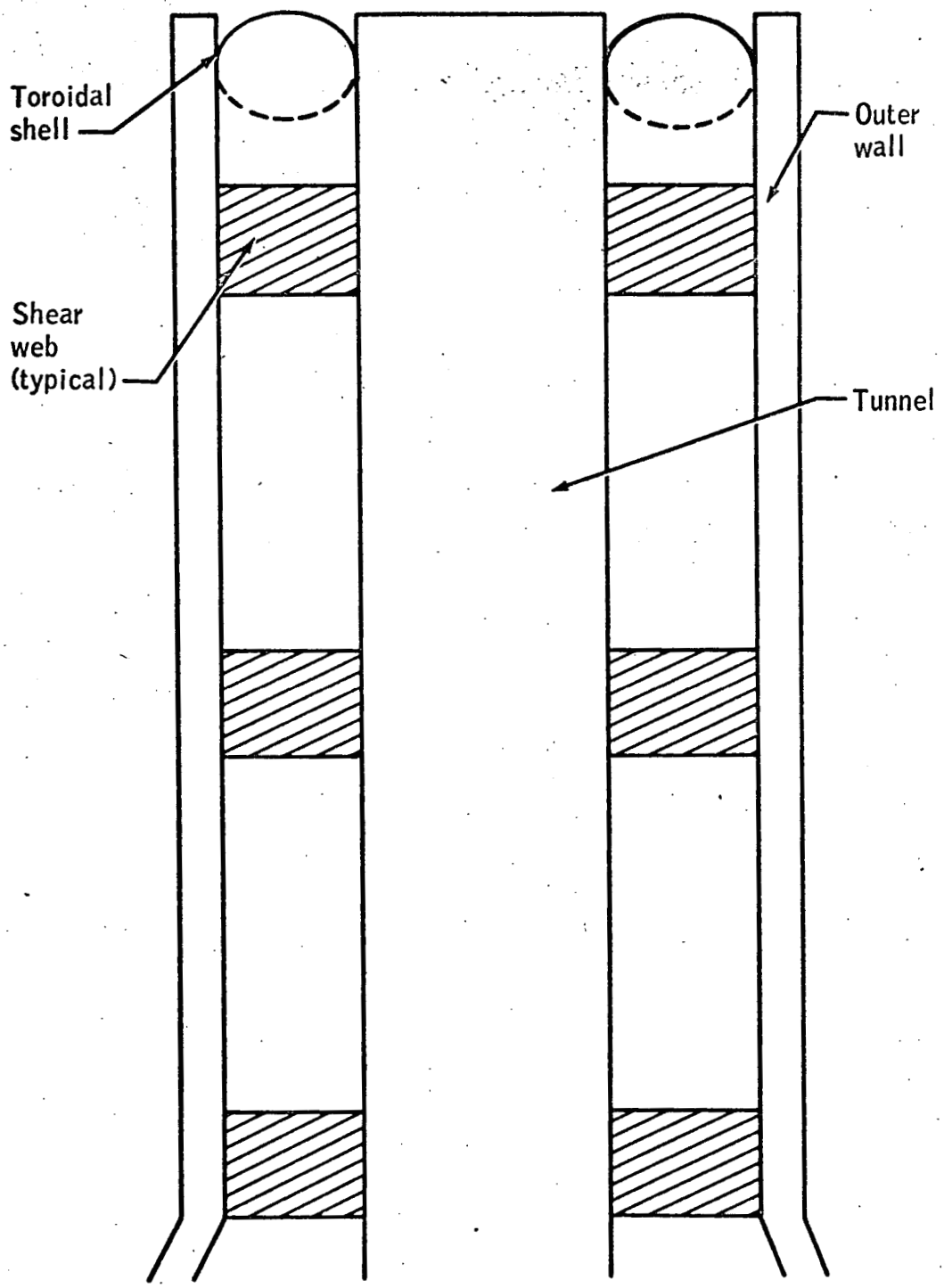

Figure 13.- Toroidal shell with shear webs.

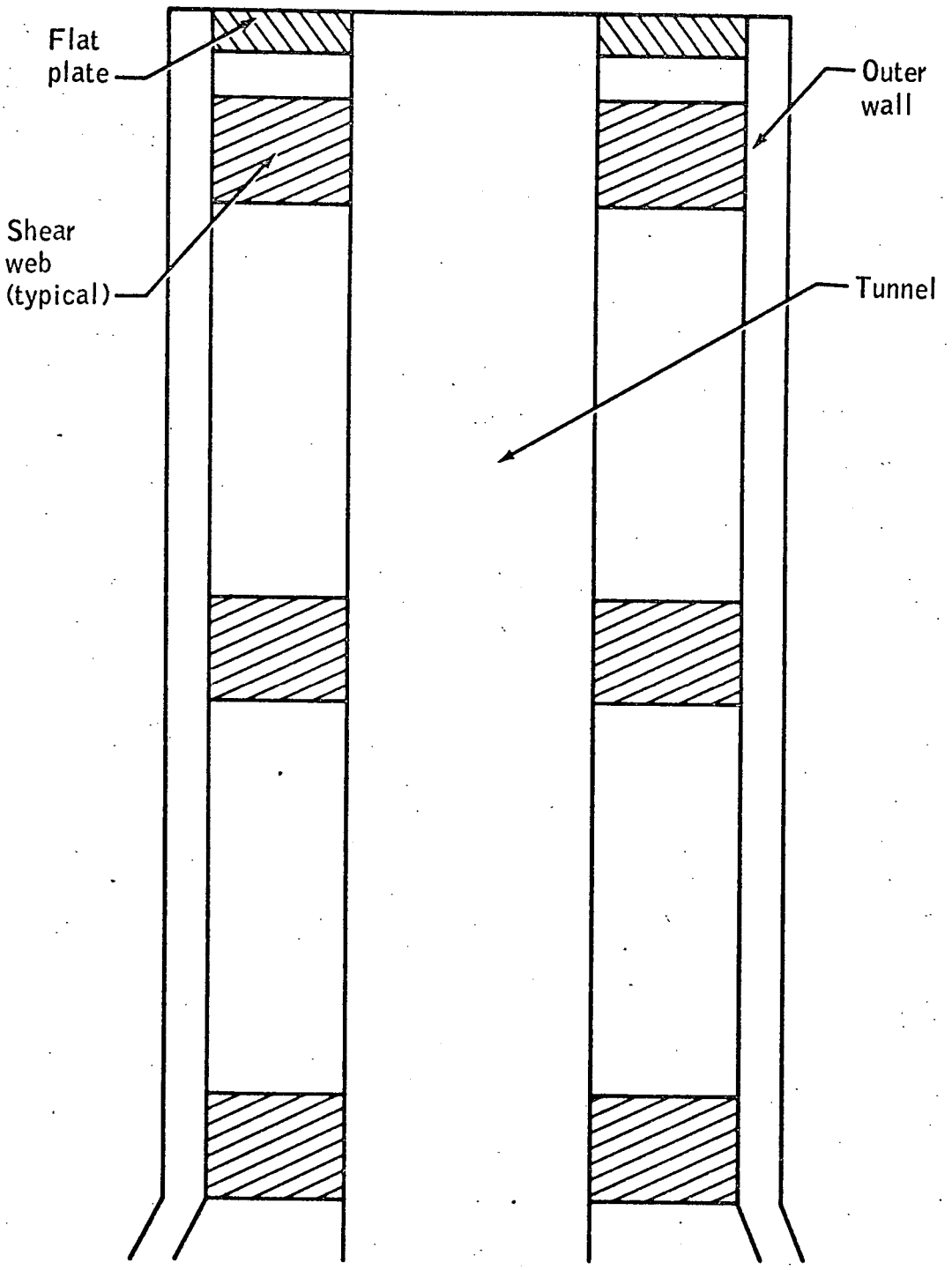

Figure 14.- Flat plate with shear webs.

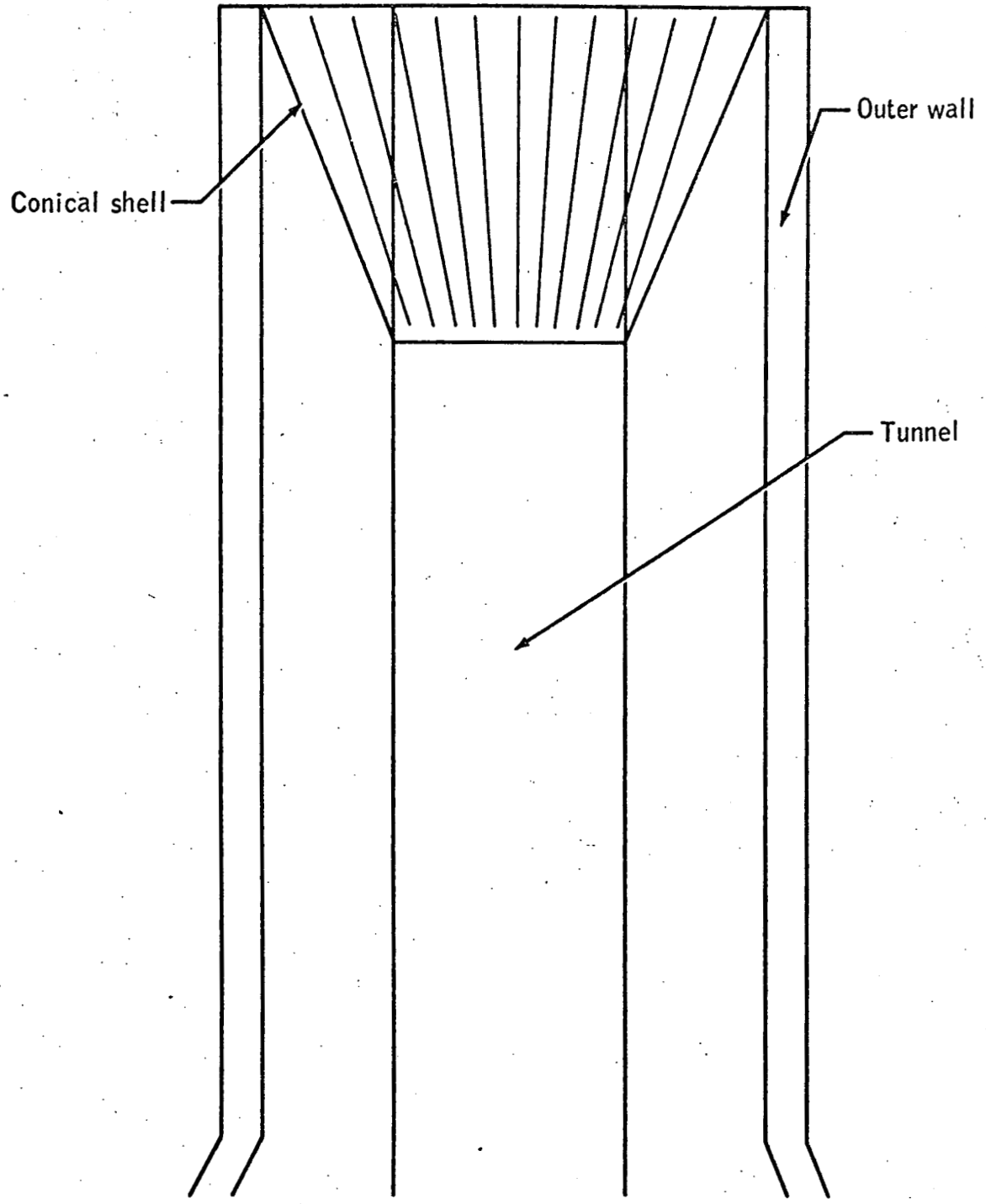

Figure 15.- Conical shell.

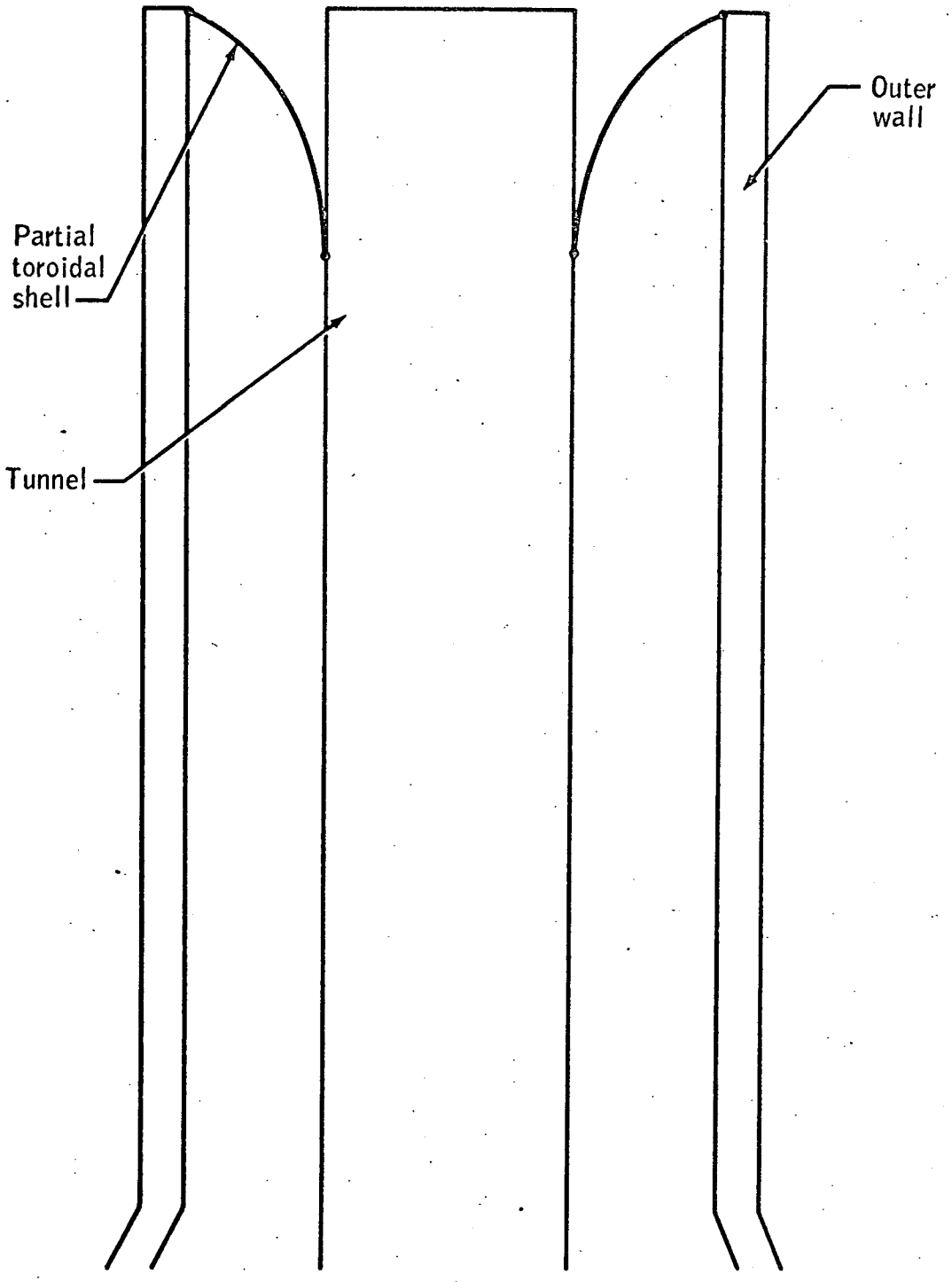

Figure 16.- Partial toroidal shell.

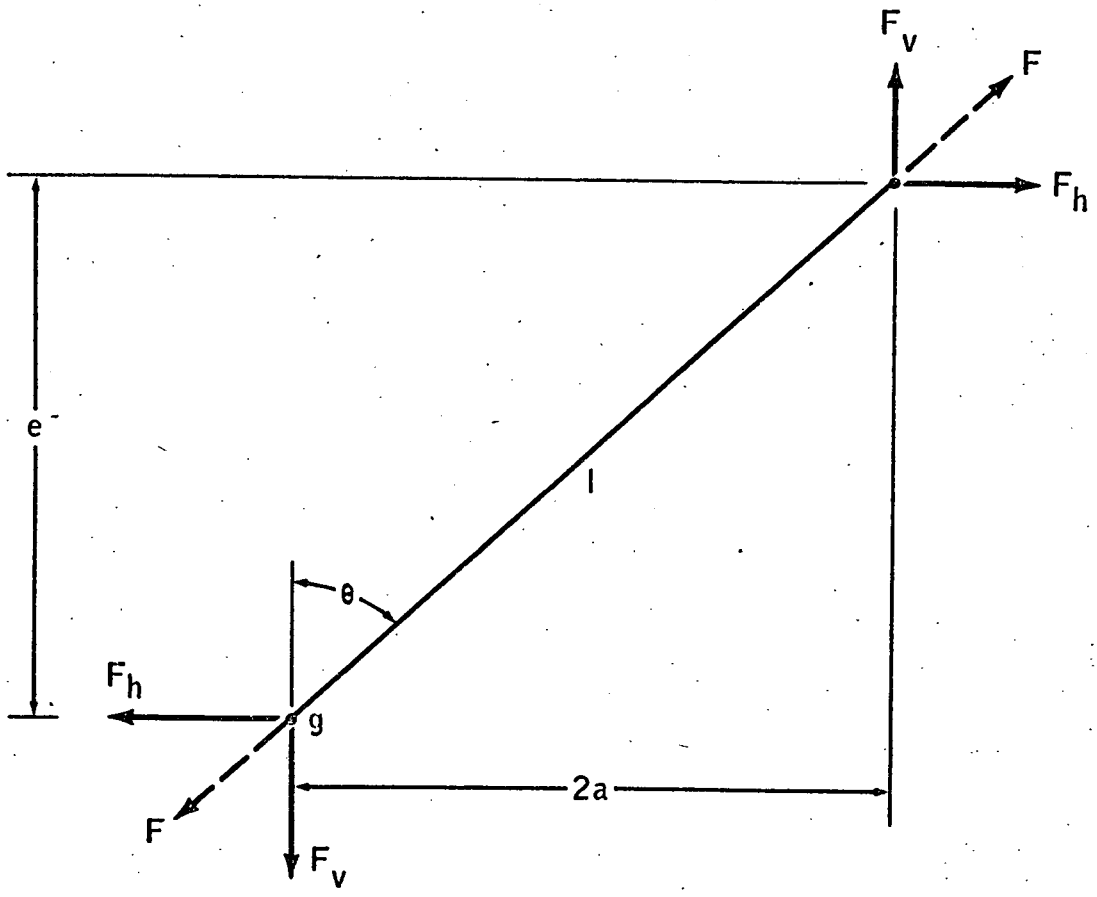

Figure 17.- Free-body diagram, tension rod.

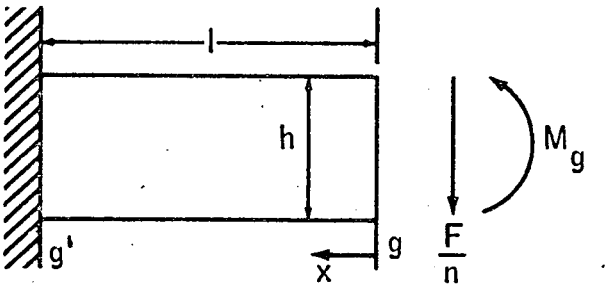

Figure 18.- Shear web.

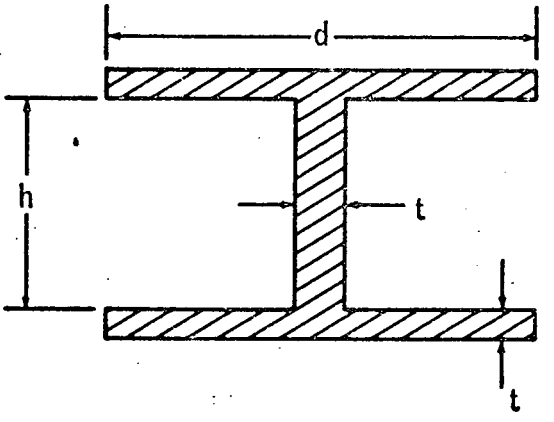

Figure 19.- Shear-web geometry.

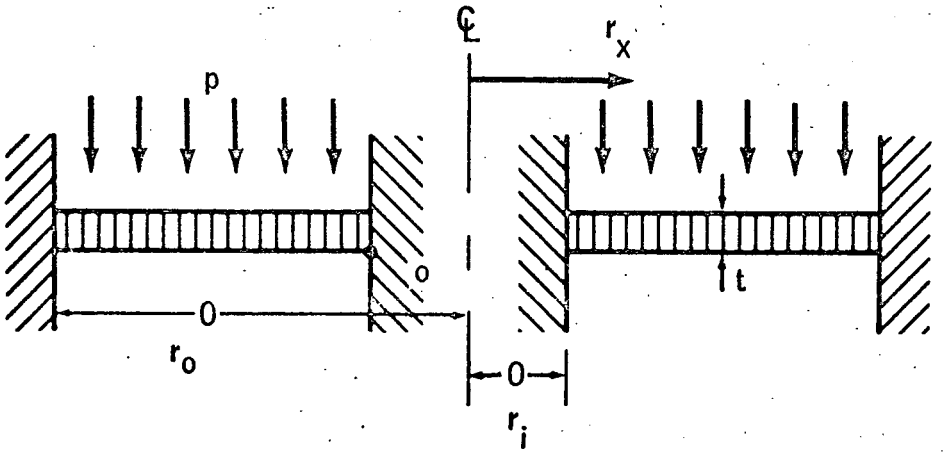

Figure 20.- Flat-plate bulkhead (solid plate).

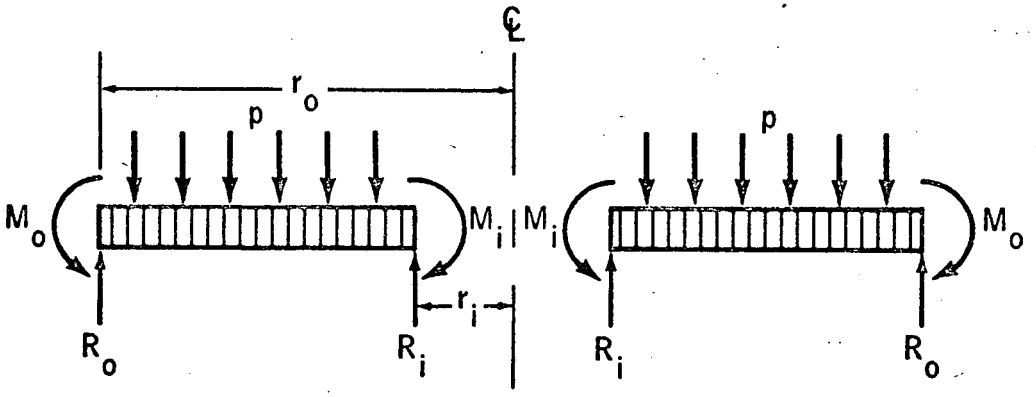

Figure 21.- Free-body diagram, flat-plate bulkhead (sandwich plate).

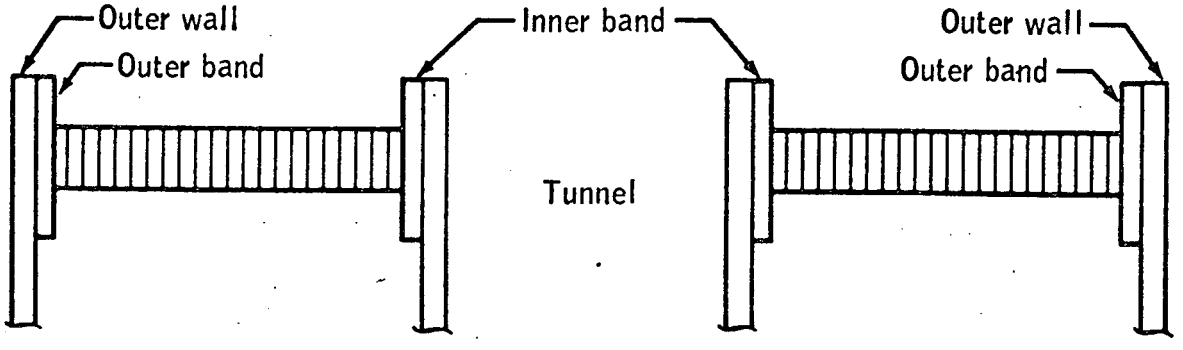

Figure 22.- Flat-plate closure.

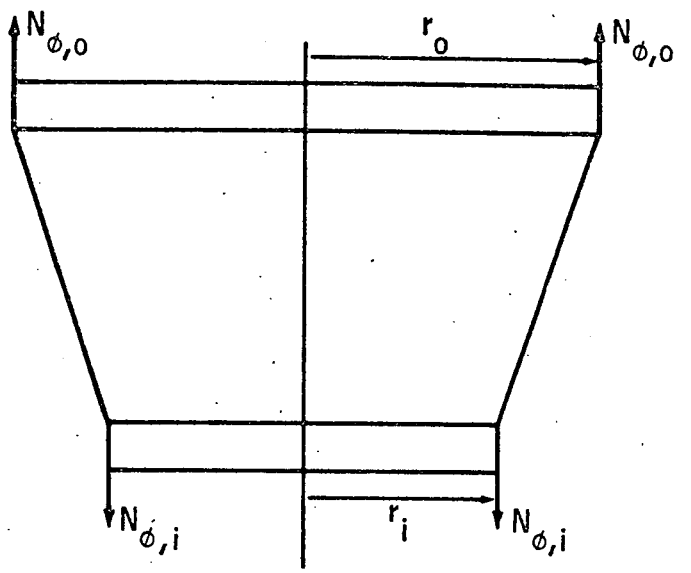

Figure 23.- Conical-shell-closure geometry.

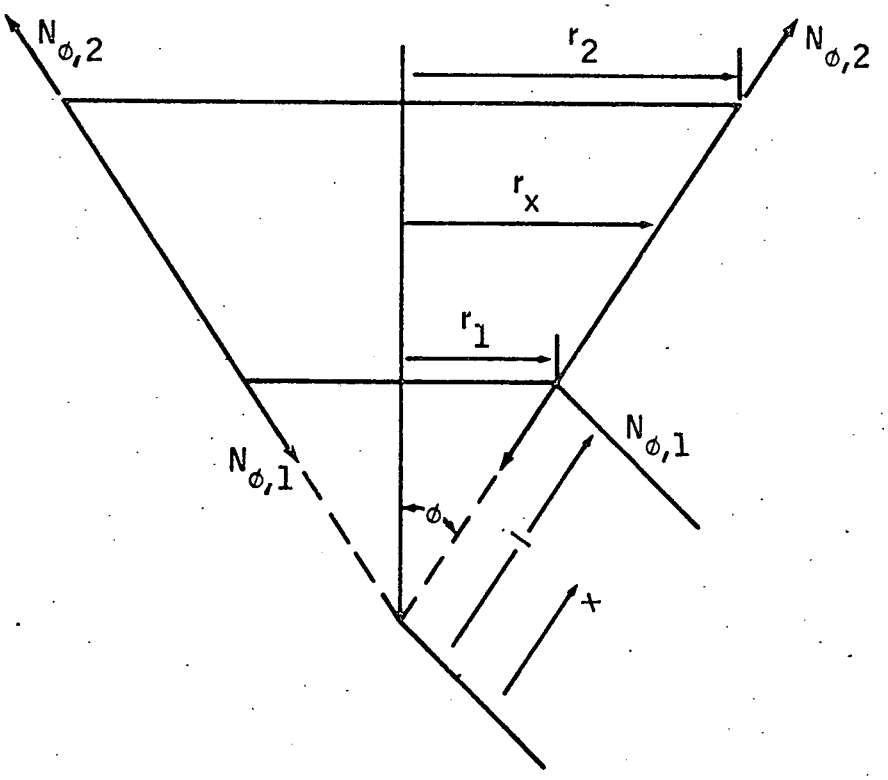

Figure 24.- Free-body diagram, cone.

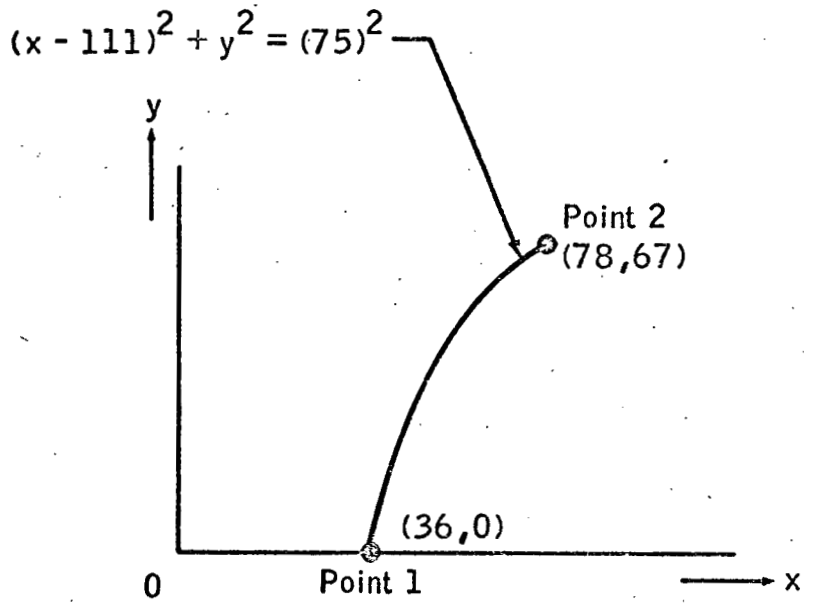

Figure 25.- Surface area, partial torus.

NASA — MSC — Coml., Houston, Texas